M.Sc. Thesis
Meteorology

THE VERTICAL PROFILES OF TEMPERATURE AND RELATIVE HUMIDITY ASSOCIATED WITH DEEP CONVECTION OVER TROPICAL OCEANS

Meri Virman

2.10.2015

Supervisors: Doc. Marja Bister
Dr Victoria Sinclair

Reviewers: Prof. Heikki Järvinen
Doc. Marja Bister

UNIVERSITY OF HELSINKI
DEPARTMENT OF PHYSICS

P.O. BOX 64 (Gustaf Hällströmin katu 2)
FIN-00014 University of Helsinki

HELSINGIN YLIOPISTO – HELSINGFORS UNIVERSITET – UNIVERSITY OF HELSINKI

Tiedekunta/Osasto – Fakultet/Sektion – Faculty/Section	Laitos – Institution – Department	
Tekijä – Författare – Author		
Työn nimi – Arbetets titel – Title		
Oppiaine – Läroämne – Subject		
Työn laji – Arbetets art – Level	Aika – Datum – Month and year	Sivumäärä – Sidoantal – Number of pages
Tiivistelmä – Referat – Abstract		
Avainsanat – Nyckelord – Keywords		
Säilytyspaikka – Förvaringställe – Where deposited		
Muita tietoja – Övriga uppgifter – Additional information		

HELSINGIN YLIOPISTO – HELSINGFORS UNIVERSITET – UNIVERSITY OF HELSINKI

Tiedekunta/Osasto – Fakultet/Sektion – Faculty/Section	Laitos – Institution – Department	
Tekijä – Författare – Author		
Työn nimi – Arbetets titel – Title		
Oppiaine – Läroämne – Subject		
Työn laji – Arbetets art – Level	Aika – Datum – Month and year	Sivumäärä – Sidoantal – Number of pages
Tiivistelmä – Referat – Abstract		
Avainsanat – Nyckelord – Keywords		
Säilytyspaikka – Förvaringställe – Where deposited		
Muita tietoja – Övriga uppgifter – Additional information		

CONTENTS

1 INTRODUCTION

A large part of global total precipitation occurs in tropical regions near the equator (Hartmann 1994, p.121). Over these regions, most of the rainfall comes from convective systems instead of synoptic scale baroclinic weather disturbances that produce most of the precipitation in midlatitudes. Convective clouds have a tendency to produce intense rainfall. Intense showers, flooding and thunder can have large impact on local society and environment. Therefore, the importance of producing accurate numerical forecast of the intensity, timing and location of precipitating convective clouds and systems cannot be overstated. In order to produce accurate forecasts, the physics of deep convection need to be understood and parameterized based on the understanding. This on the other hand depends crucially on how well the factors affecting the behaviour of tropical deep convection are known and how well the mechanism by which they affect is understood.

According to the classical convection theory, deep moist convection depends on humidity and temperature in the planetary boundary layer (PBL), as well as the temperature in the free-troposphere (Bister 2014). However, the classical convection theory doesn't explain any sensitivity to free-tropospheric humidity. Both observations and modeling studies suggest that, at least in the tropics, deep moist convection depends crucially on humidity above the PBL (Holloway and Neelin 2009, Sobel et al. 2004, Bretherton et al. 2004, James and Markowski 2010). Sobel et al. (2004) investigated convection over Kwajalein atoll and came to the conclusion that deep convection and relative humidity (RH) correlate so that high lower-tropospheric RH favors subsequent convection. Holloway and Neelin (2009) conditionally averaged humidity profiles with the amount of precipitation and found that there is an increase in precipitation with high enough partial column water vapor in the 800-250 hPa layer. Bretherton et al. (2004) predicted precipitation with column-RH and concluded that the observed and predicted precipitation were almost exactly in phase. These are just few of the studies that have concluded that free-tropospheric humidity has an important role in the transition from shallow to deep convection. The

mechanism by which free-tropospheric humidity affects deep convection is not fully known, but the sensitivity is often explained with entrainment of environmental air to the cloud or by the effect of downdrafts driven by evaporation of rain (Bister 2014). Understanding the mechanism by which humidity above the PBL controls deep convection is of crucial importance for convective parameterization.

In the tropics, mean horizontal temperature gradients are small and the average water content is high. Because the behavior of deep convection depends on the vertical profiles of temperature and RH, it is important to know which processes cause anomalies of temperature and RH in the tropics. It has been hypothesized recently that it is the moistening effect of cumulus congestus clouds, which populate the midlevels of the atmosphere in the tropics, that leads to the initiation of deep convection. However, the time-scale analysis of Hohenegger and Stevens (2013) showed that congestus clouds moisten the atmosphere too slowly to have a significant effect on the transition to deep convection. One other important process is deep convection itself. Deep convection occurs frequently in the tropics and it can be associated with intense condensation, freezing, evaporation and melting. Water vapor ascending in the strong updrafts condenses to form new cloud droplets and precipitation. Falling rain droplets evaporate in the unsaturated air below the cloud. Because condensation causes diabatic heating and evaporation cools the atmosphere, convective clouds can cause significant changes to the temperature and humidity fields. The temperature anomalies then spread to the surrounding environment via gravity waves. Therefore, deep convection itself is an important process that produces anomalies of temperature and humidity. However, because convection depends on these anomalies, they are of crucial importance for subsequent convection.

This study will investigate, by analysing radiosonde data from six stations over the eastern Indian Ocean, maritime Southeast Asia and western Pacific, how convection occurring as mesoscale convective systems (MCSs) influences the vertical profiles of temperature and RH. The results of the relationship between precipitation and temperature and RH, especially in the lower part of the

troposphere, can be of important use in making assumptions on how the convection, through induced changes in the vertical profiles of temperature and RH, can affect subsequent convection.

Chapter 2 describes the climatology of precipitation in the tropics and provides further insight into the formation and structure of MCSs. Chapter 3 describes the data and methods used in this study to investigate the effects of precipitation. In chapter 4, the results obtained by analyzing radiosonde and precipitation data over tropical oceans are presented. In chapter 5, the results obtained in this study and their relation to other studies and to subsequent convection is discussed.

2 BACKGROUND

In this chapter, a discussion of the climatology of precipitation in the tropics is provided to better understand where the effects of precipitation are most significant (section 2.1). This will also provide reasoning for why the specific stations in this study were selected (chapter 3). After this we will investigate the observed structure and effect of MCSs based on other studies in order to better understand how organized convection modifies the vertical profiles of temperature and humidity (section 2.2).

2.1 Climatology of precipitation in the tropics

Figure 1 shows the mean total precipitation in the tropics. Over the Pacific and tropical Atlantic Ocean near the equator, there is a narrow region of high precipitation rate, the Intertropical Convergence Zone (ITCZ). ITCZ forms where the northeast and southeast trade winds converge and is located slightly to the north of the equator during both northern hemisphere summer and winter. Most precipitation falls over the maritime continent and Melanesia. The eastern part of this high precipitation region extends to southeast and is called the South Pacific Convergence Zone (SPCZ). During the northern hemisphere

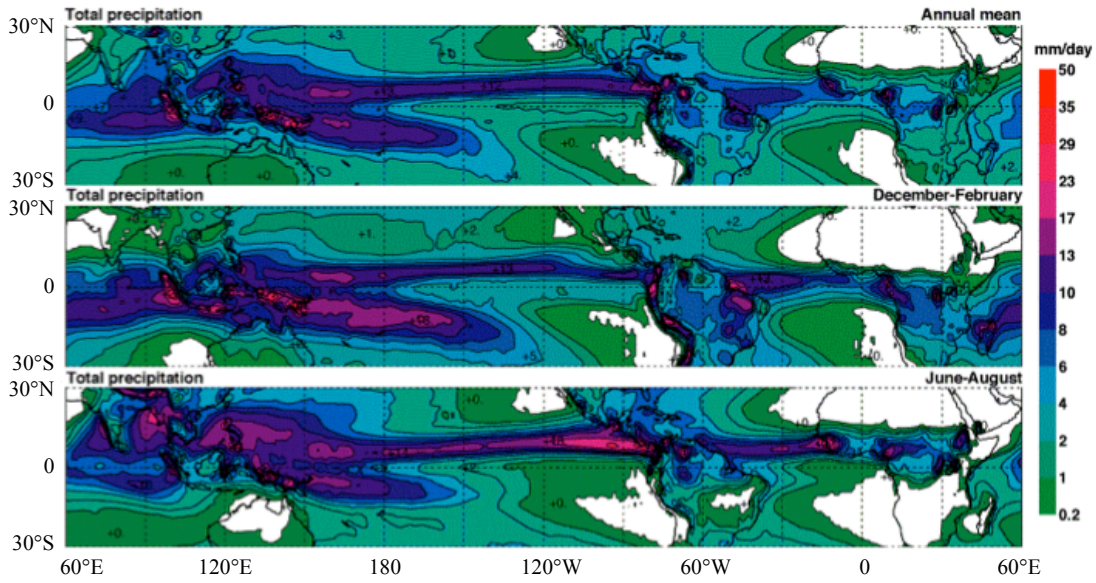

Figure 1. *Mean surface total precipitation between latitudes 30°N/S from the ERA-40 reanalysis data. Precipitation is in units of mm/day and it is calculated from September 1957 – August 2002. Upper panel is the annual mean, middle panel is the December-February mean and in the lower panel is the June-August mean precipitation. Image is provided by the European Centre for Medium-Range Weather Forecasts (ECMWF).*

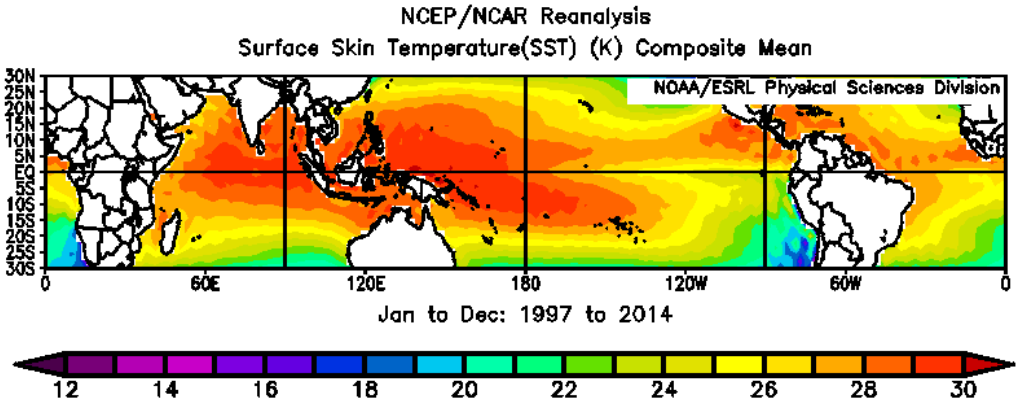

Figure 2. Mean horizontal sea surface temperature (SST) distribution in units of Celsius between latitudes 30°N/S from the NCEP/NCAR Reanalysis dataset (Kalnay et al. 1996). Composite mean is constructed from the time period of January-December 1997-2014. Image is provided by the NOAA/ESRL Physical Sciences Division.

summer there is a maximum of precipitation over the southern and southeast Asia. During the northern hemisphere winter the maximum precipitation occurs over South-America, Africa and the northern Australia. Over the eastern Indian Ocean heavy precipitation occurs mostly during northern hemisphere winter.

Figure 2 shows the mean horizontal sea surface temperature (SST) distribution in the tropics. The western Pacific is commonly referred to as the "warm pool" (Lucas and Zipser, 2000), since SST in this region is large throughout the year (figure 2). A narrow region of high SST is seen over the equatorial Pacific in the regions of the ITCZ. In the eastern Indian Ocean SST is large during northern hemisphere winter (not shown). Comparison of figures 1 and 2 shows that regions of high SST and large amounts of precipitation are co-located. Convective activity is indeed known to be largest over the regions of large SSTs. Therefore, over the western Pacific and eastern Indian Ocean, most of the precipitation is associated with deep convection. The maximum of precipitation in the southeast-Asia during northern hemisphere summer and the maxima in the South-America, Africa and northern Australia in the northern hemisphere winter are mostly due to the effect of monsoon convection.

Rickenbach and Rutledge (1998) studied the occurrence frequency and rainfall production of MCSs observed during TOGA COARE (Tropical Ocean Global Atmosphere Coupled Ocean-Atmosphere Response Experiment). TOGA COARE –field experiment studied atmospheric and oceanic processes over the region of the western Pacific in 1992-1993. According to Rickenbach and Rutledge, observations made during the campaign show that over 80 % of total rainfall was associated with MCSs and only 12 % was associated with systems of isolated cells. According to satellite observations, MCSs over the oceanic warm pool occur mostly as inseparable "superclusters" (Mapes 1993). The heating profiles and other thermodynamic effects of organized convection differ from those of individual precipitating convective clouds. Because MCSs often occur in the tropics, a more detailed discussion of the observed structure, life cycle and effect of MCSs is presented next.

2.2 Mesoscale convective systems

To understand the effect that convection organized as MCSs has on the vertical profiles of temperature and RH, one requires knowledge of the life cycle and structure of MCSs. This section first describes the lifecycle and structure of

MCSs based on literature (section 2.2.1). In section 2.2.1 the author is referencing the book by Houze (1993) and citations therein unless otherwise noted. After this, the observed processes occurring in MCSs and how they have been observed to affect the heating profiles of MCSs (section 2.2.2) and the occurrence of downdrafts (section 2.2.3) is discussed based on previous literature.

2.2.1 Structure and life cycle

MCSs are defined as cloud systems where the area of contiguous precipitation is 100 km or more in horizontal scale in at least one direction. MCSs consist of convective and stratiform cloud types. Both cumulonimbus and congestus clouds form the convective areas of MCSs. The deep convective clouds spread to the surroundings in the upper troposphere and form an anvil cloud that produces stratiform precipitation.

MCSs occur in many forms and sizes. Roughly two types of MCSs can be distinguished based on where convection occurs relative to stratiform precipitation. In MCSs of the first type, deep convection occurs as a squall line in the front of the system and stratiform rainfall covers areas behind the line of convection. Convection in the second type of MCSs occurs as separated and randomly located towers and in between these towers are the stratiform rain areas.

The lifecycle of an MCS begins with the development of individual cumulonimbus towers. The tops of these towers are located at 200 hPa or higher (Zipser 1977). Strongest updrafts also occur in the cumulonimbus towers. As the cumulonimbus clouds reach the tropopause, they cannot grow through this stable layer and therefore the cloud spreads to the surroundings in the upper troposphere and forms the anvil cloud. After some time, the anvil clouds of separate cumulonimbus clouds merge. This extensive region of stratiform precipitation can be as large as 200 km in horizontal dimension. The merged and mature anvil cloud mass is observed to be usually about 6-10 km

thick and its lower boundary is located between 500 and 600 hPa (Zipser 1977). New cumulonimbus towers continuously form as the older towers weaken and their associated anvil clouds spread in the horizontal dimension. MCSs therefore always consist of both active and weakening cumulonimbus cells and the associated anvil cloud mass. At some point, the formation and growth of new cells diminishes, leaving behind only a weakening anvil cloud mass. The duration of this cycle and the lifetime of MCSs varies from 10 hours to 2-3 days.

2.2.2 Diabatic heating

The deep convective cloud and anvil cloud in MCSs are associated with different kind of vertical profiles of diabatic heating. Intense condensation of water vapour within the vertically deep cumulonimbus clouds causes diabatic heating throughout the free-troposphere. Diabatic heating associated with the anvil cloud extends from roughly 500-600 hPa to the tropopause. Evaporation of precipitation falling from the anvil cloud causes diabatic cooling below the anvil cloud. The temperature anomalies associated with diabatic cooling and diabatic heating spread to the surrounding environment with gravity waves.

The velocity by which the gravity waves disperse the temperature anomalies depends on how deep the heating or cooling is (Mapes and Houze 1995). Mapes and Houze (1995) studied the diabatic divergence profiles in Western Pacific MCSs using a hydrostatic and motionless model in which wind speed and the coriolis parameter were 0. They induced a heating profile similar to the observed heating profiles of MCSs at time 0 and investigated the resulting temperature field that prevails 6 hours after the start of heating (figure 3). According to Mapes and Houze, the positive temperature anomaly induced by the diabatic heating in the deep convective cumulonimbus cloud propagates at speed of roughly 35-50 ms^{-1}. Both the positive and negative temperature anomalies induced by the diabatic heating in the anvil cloud and diabatic cooling due to the evaporation of precipitation falling from the anvil cloud propagate slower, at roughly 15-25 ms^{-1}. Therefore, deeper vertical structures propagate faster. The temperature anomalies induced by the deep convective

cumulonimbus and anvil cloud can be distinguished in figure 3. Figure 3 shows that the temperature anomalies can be over 1°C. Temperature anomalies of this size can have significant impact on subsequent convection.

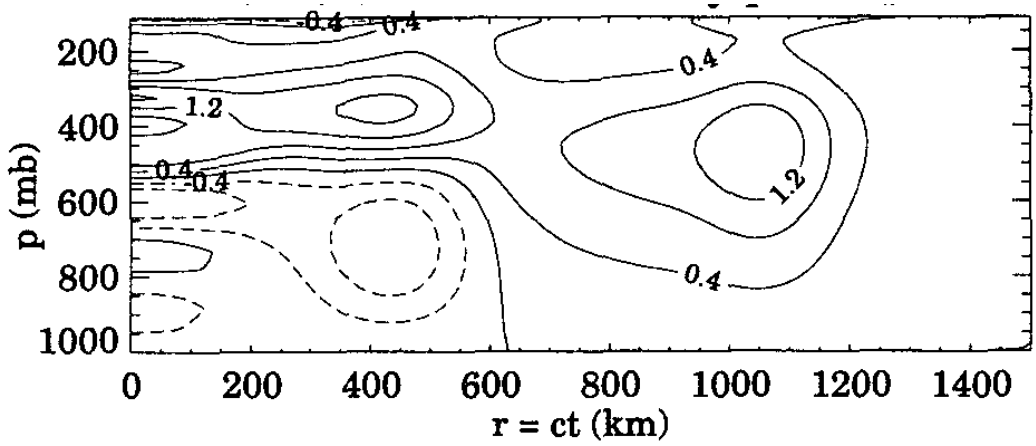

Figure 3. *Temperature perturbation field six hours after the initiation of an imposed heat source similar to that induced by MCSs. Contour interval is 0.4°C and negative contours are dotted. Figure is from Mapes and Houze (1995). The model and induced heating profile is discussed in more detail in their study.*

2.2.3 Downdrafts

In addition to the diabatic effect of condensation/freezing and evaporation/melting, also other processes within MCSs can modify the temperature and moisture field of the atmosphere. Zipser (1977) studied the characteristics of squall-line type MCSs mainly over tropical oceans. They gathered observations obtained from aircraft penetrations as well as satellite data, radar data, surface meteorological data and radiosonde measurements conducted ahead and behind the squall lines. They concluded that, based on soundings made in the post-squall region, the lowest layer near the surface was occupied by cool, near-saturated air (figure 4). Figure 4 also shows that in all soundings, a stable layer separates this cool and moist air from relatively warm and drier air just above. The maximum difference between the temperature and dew point temperature in the whole troposphere is 15°C, usually near 900 hPa, which is also where the warmest air is observed. When the sounding approached the base of the anvil, the moisture content of air rose. On average,

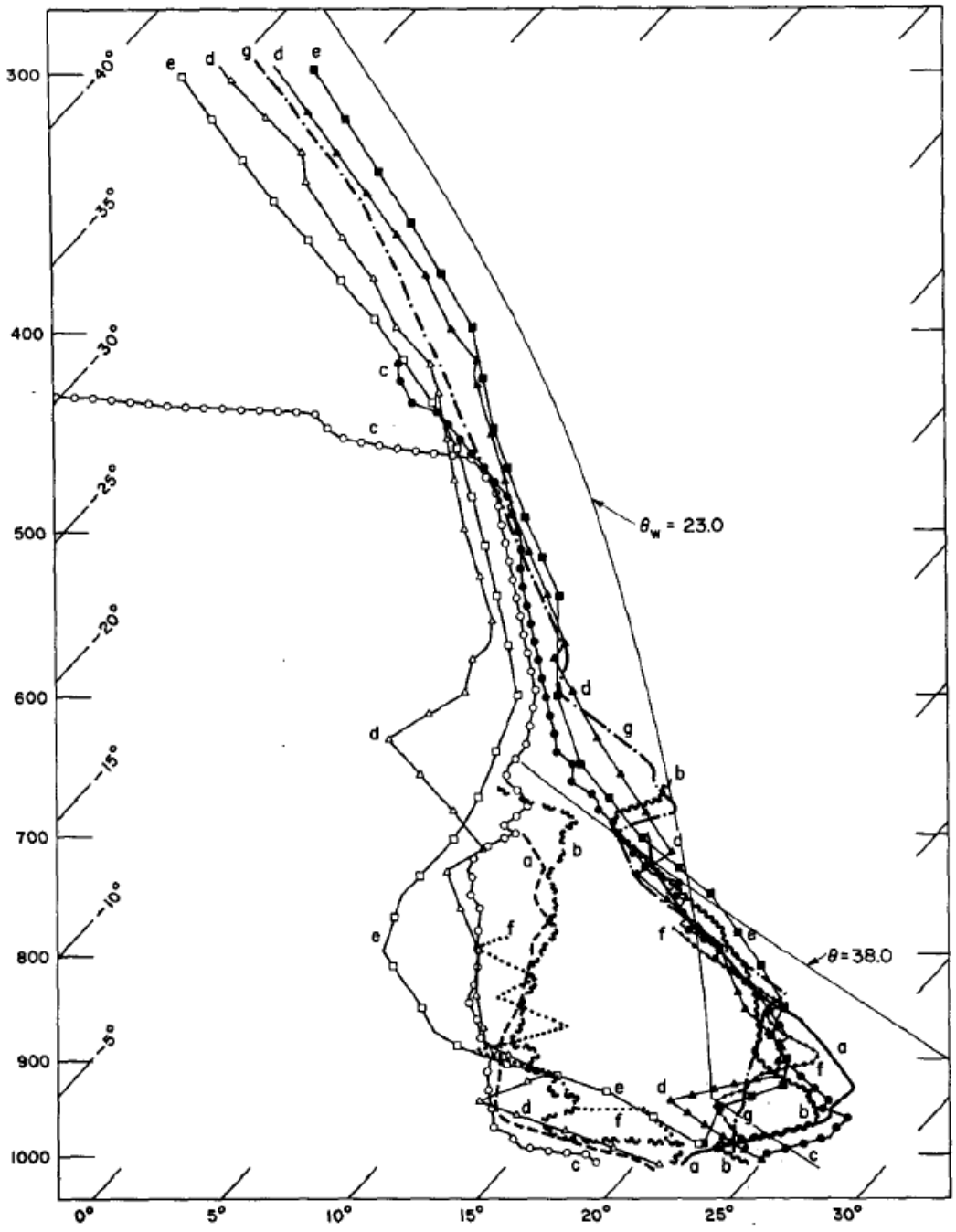

Figure 4. *Soundings made in post-squall regions of different MCSs. Figure is from Zipser (1977). See their figure 8 and its caption for description of the location and measurement time of the soundings and position of the soundings relative to the squall line.*

the temperature and dew point temperature curves approached each other at roughly 600 hPa, which indicates the base of the anvil cloud.

According to Zipser, the observed temperature and dew point temperature profiles within the MCSs were the result of two distinct types of downdrafts, mesoscale unsaturated downdrafts and convective-scale saturated downdrafts. They hypothesized that the dry air found behind the squall line above the coolest layer near the surface had to originate from above 700 hPa. According to Zipser, this air must have descended in mesoscale unsaturated downdrafts under the influence of evaporation of stratiform rain. Zipser also reasoned that the coolest air found in the lowest layer had to be the result of convective-scale saturated downdrafts that occur in the region of the deep convective cumulonimbus cloud. The convective-scale saturated downdrafts are so intense they can spread far from the cumulonimbus cells near the surface.

3 DATA AND METHODS

This chapter describes the data and methods used in this study to provide information of the relationship between deep convection and humidity and temperature in the troposphere. First, the data used in this study will be described (section 3.1). Then, a discussion of how the data was processed and classified to give information of the relationship of precipitation with temperature and humidity is provided (section 3.2). The data was analyzed with the numerical computing environment and programming language MATLAB.

3.1 Data

To investigate the relationship between deep convection and the vertical profiles of temperature and RH it is reasonable so study areas where it precipitates often and most precipitation is occurring with MCSs. As explained in chapter 2, most precipitation occur in the region of Southeast Asia, Melanesia, eastern Indian Ocean and northern parts of Australia. Six stations in the maritime Southeast Asia, Indian Ocean and western Pacific were selected and they are located in Funafuti, Darwin, Gove, Singapore, Thiruvananthapuram and Diego Garcia (figure 5). This research first began with studying precipitation

associated with the Madden-Julian -oscillation (MJO). The abovementioned stations were initially selected because their data record was long, they were in the right area with respect to the occurrence of MJO and they were found in the Integrated Global Radiosonde Archive (IGRA). Because there are only a limited number of measuring stations in the tropics, the number of stations that fill the aforementioned criteria is small.

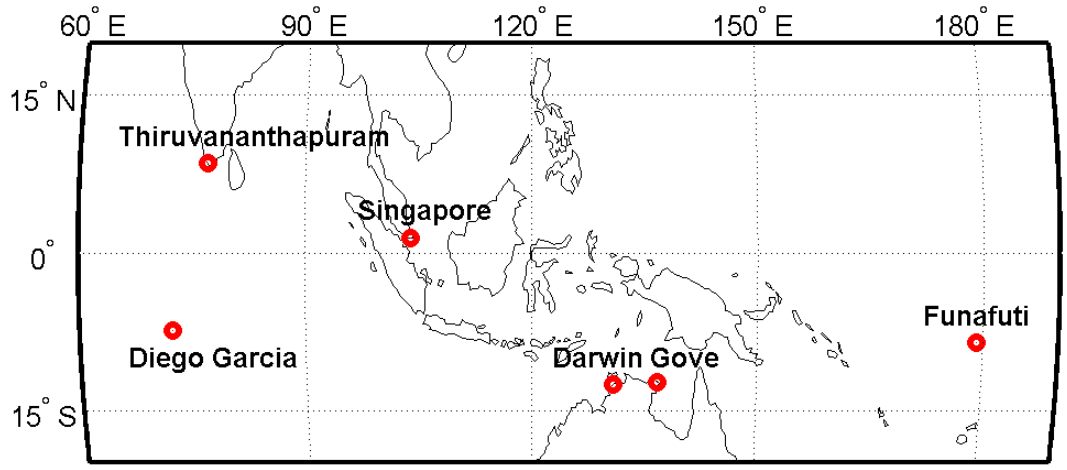

Figure 5. *Location of the stations (red) from where radiosonde data is analysed.*

Time period of investigation was selected to be from November-February 1997 to 2014. During the southern hemisphere summer the amount of precipitation over the investigated area (figure 1) is large and this was the main reason for these months to be selected.

3.1.1 Integrated Global Radiosonde Archive

Atmospheric soundings are common in-situ measurements that provide information of the vertical distribution of different physical properties. Therefore, in order to study the relationship between precipitation and the vertical profiles of temperature and RH, we chose to study soundings. The soundings analysed in this study were obtained from the Integrated Global Radiosonde Archive (IGRA, https://www.ncdc.noaa.gov/data-access/weather-balloon/integrated-global-radiosonde-archive). This archive contains a collection of both historical and near-real-time radiosonde observations from

around the globe and have been made available by the NOAA National Centers for Environmental Information. The archive contains three components: quality-assured individual soundings, monthly means and sounding-derived humidity and stability parameters, the first of which were examined in this study. The quality assured individual soundings provide observations of temperature, dew point depression, wind direction and wind speed.

The soundings are provided in the archive so that only observations from mandatory and significant levels are available. Mandatory pressure levels are those specified by the World Meteorological Organization in 1997 and are 1000, 925, 850, 700, 500, 400, 300, 250, 200, 150, 100, 70, 50, 30, 20 and 10 hPa. Significant levels are defined as levels at which a significant change in the variable in question occurred. Between these and/or the mandatory levels the variable changed linearly with height. The variables provided at these levels are temperature and dew point depression. Wind speed and wind direction are provided at significant, mandatory and at additional wind levels. Additional wind levels are levels from which only observations of wind speed and wind direction exists.

3.1.2 Tropical Rainfall Measuring Mission

Precipitation observations used in this study were provided by the Tropical Rainfall Measuring Mission (TRMM, http://trmm.gsfc.nasa.gov/). TRMM is a joint mission between NASA and the Japan Aerospace Exploration Agency and is designed to monitor and study tropical rainfall. Their archive contains quasi-global, near-real-time, TRMM-based precipitation estimates for the research community. The estimates are derived from satellites and are provided on a 0.25°x0.25° grid over the latitude band 50°N/S within seven hours of observation time. We have used their daily precipitation product that is in units of mm/day and is the sum of precipitation observed in a time period that starts at 22:30 UTC and ends at 22:30 UTC the next day.

3.1.3 Temporal resolution

Figure 6 visualizes how the temporal resolution of the TRMM-based precipitation estimates and radiosonde measurements relate to each other. The temporal resolution of radiosonde observations varied between the stations: in some stations observations were made every 24 hours whereas in some every 12 hours. In Funafuti radiosonde observations were usually made every 24 hours and at 23 or 00 UTC at most cases. Precipitation values are always the sum of precipitation from 24 hours before the radiosonde observation. Therefore, the temporal resolution in this study is 24 hours.

3.2 Methods

In this chapter a discussion of how the data provided by IGRA and TRMM was processed to determine the relationship of precipitation with different atmospheric quantities is presented.

Since the soundings were provided only at certain levels and we are interested in a more dense vertical resolution, observations were interpolated in the vertical. Coherent temperature, dew point temperature and wind speed profiles for all soundings were produced by linear interpolation every 1 hPa between the mandatory, significant and additional wind levels.

RH is the ratio of mixing ratio to saturation mixing ratio and it is expressed in percent. RH was chosen to be the moisture quantity investigated in this study because this variable depends on the absolute moisture content as well as temperature in the atmosphere and it gives information of the saturation state of the atmosphere. RH was calculated with respect to water, because it is not known at which altitudes and when water droplets freeze. When RH with respect to water reaches 100 %, water vapour condenses and the formation of cloud droplets begins. RH was calculated using the definition in Rogers and Yau (1989):

$$RH = 100\frac{w}{w_s},$$

where w and w_s are the mixing ratio and saturation mixing ratio of water vapour in units of kg/kg. They were calculated using the following formulae from Rogers and Yau (1989):

$$w = \frac{\varepsilon}{p} A \exp\left(\frac{-B}{T_d}\right),$$

$$w_s = \frac{\varepsilon}{p} A \exp\left(\frac{-B}{T}\right),$$

where $\varepsilon = 0.622$, $A = 2.53 \times 10^8$ kPa, $B = 5.42 \times 10^3$ K, p is pressure, T_d is dew point temperature and T is temperature. Dew point temperature is calculated from the dew point depression which is defined as T- T_d. Using the interpolated values of temperature and dew point depression at all pressure levels a vertical profile of RH for every sounding was constructed.

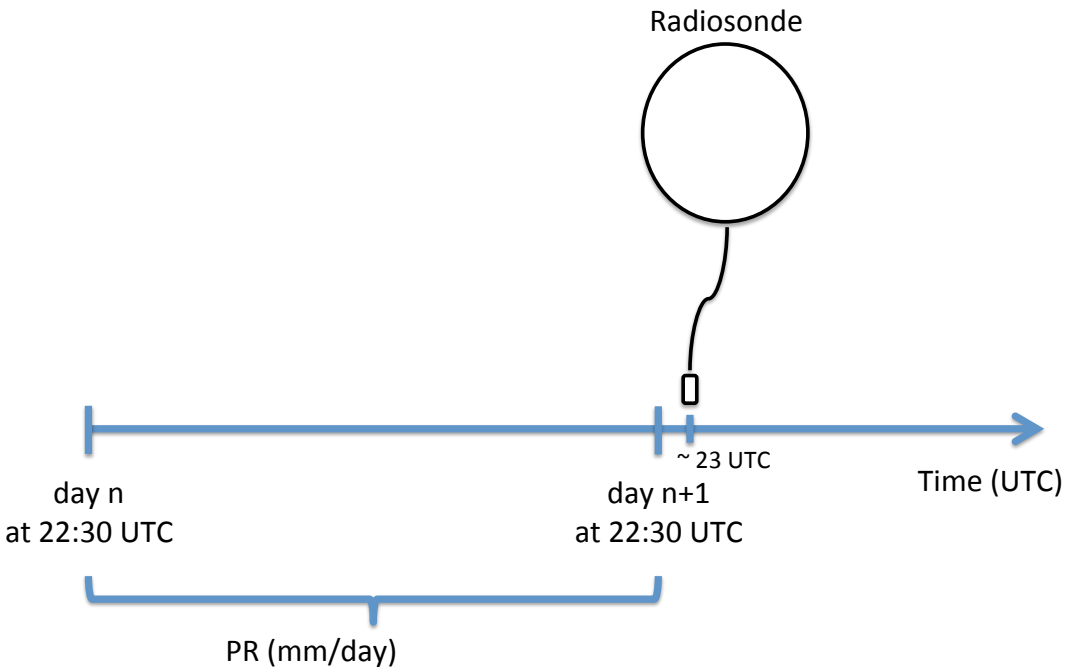

Figure 6. *Demonstration of the temporal resolution in this study. All values of precipitation (PR) are always calculated from a time period of 24 hours before the radiosonde measurement.*

For each station, soundings were binned based on the amount of precipitation obtained during the previous 24 hours to investigate how the amount of precipitation is related to the temperature and RH structure in the atmosphere. The area-averaged precipitation was calculated for every day in the investigated time period by taking the mean of precipitation values from the nearest 16 grid cells to the station. This way, the station is in the centre of the area and the area covers 1°x1° in latitude and longitude around the station. The same was done by taking the mean of precipitation values from the nearest 400 grid cells to the station and so the area covers 5°x5° in latitude and longitude around each station. The soundings were divided into groups depending what on the amount of area-averaged precipitation during the previous 24 hours was. The groups are presented in table 1.

Table 1. *The amount of area-averaged precipitation in units of mm/day obtained during 24 hours before the radiosonde observation in the different precipitation groups (PR0-PR5).*

Group name	PR0	PR1	PR2	PR3	PR4	PR5
Precipitation rate (mm/day)	< 1	5-10	10-15	15-20	20-25	25-30

The limit of less than 1 mm of precipitation in the group PR0 was chosen to select soundings that represent a non-precipitating atmosphere. Even though a small amount of precipitation may have occurred, this group, or the "fair weather group", can be thought to represent non-precipitating atmosphere, since precipitation amount of less than 1 mm in 24 hours is so small its effect is not significant. The rest of the groups (PR1-PR5), or "precipitation groups" contain soundings that represent atmosphere where a significant amount of precipitation occurred. The precipitation rates in the PR1-PR5 groups were chosen to increase the probability that the area is significantly covered by the anvil cloud and stratiform precipitation. No attempt has been made to separate the different types of MCSs in this study. The group with less than 1 mm of precipitation (PR0) can be used as a reference for the precipitation groups (PR1-PR5). For each group, a mean of observation values at each level was

taken. Thus, for each station and each group, a mean vertical profile of temperature, RH and wind speed was obtained.

4 RESULTS

In this chapter, a discussion of the results of the analysis of the radiosonde observations and precipitation estimates is provided. First, the number of observations in the different groups is presented (section 4.1). Second, the results of how different amounts of area-averaged precipitation from 1°x1° area is related to the vertical profiles of temperature and RH at all investigated measuring stations are presented (section 4.2). Section 4.3 discusses the sensitivity of the results to the size of the area from which the area-averaged precipitation was calculated. Lastly, the effect of advection by the horizontal wind on the results is discussed (section 4.4).

4.1 Number of soundings

Binning the data according to the amount of area-averaged precipitation yielded groups of sizes that are shown in table 2. The number of soundings in each group gives useful information of the climatology of precipitation at the station. It is also important to know over how many samples a mean was taken from in order to make meaningful assumptions of the vertical profiles in section 4.2.

Radiosonde observations from all stations except Diego Garcia extended throughout the time period investigated in this study (1997-2014). Observations from Diego Garcia were available in IGRA only until 2006. Therefore, at this station, the number of soundings in each group is relatively small (table 2).

In Funafuti and Darwin, the percentage of soundings in both the fair weather group (PR0) and the precipitation groups (PR1-PR5) is large and the amount of soundings in the precipitation groups exceed that of the fair weather group.

Table 2. *Number of soundings in each group at each station. PR0 is the fair weather group, PR1-PR5 are the area-averaged precipitation groups. Precipitation is averaged over a 1°x1° area, except when otherwise stated. The column "total" contains the total amount and fraction of soundings in the precipitation categories. The column "all" contains the total amount of all soundings investigated at each station. Amount gives the amount of soundings in each group. Percent gives the relative amount of these soundings from the overall amount of soundings studied in each station.*

Group	PR0	PR1	PR2	PR3	PR4	PR5	total	all
Funafuti								
Amount	277	134	91	50	38	34	347	1032
Percent (%)	26,8	13,0	8,8	4,8	3,7	3,3	33,6	100
Funafuti 5°x5°								
Amount	130	201	118	79	49	34	481	1032
Percent (%)	12,6	19,5	11,4	7,7	4,7	3,3	46,6	100
Darwin								
Amount	577	261	165	136	82	63	707	1905
Percent (%)	30,3	13,7	8,7	7,1	4,3	3,3	37,1	100
Gove								
Amount	909	182	118	73	44	30	447	1864
Percent (%)	48,8	9,8	6,3	3,9	2,4	1,6	24,0	100
Singapore								
Amount	734	245	108	81	48	44	526	1940
Percent (%)	37,8	12,6	5,6	4,2	2,5	2,3	27,1	100
Thiruvananthapuram								
Amount	970	79	47	25	15	5	171	1426
Percent (%)	68,0	5,5	3,3	1,8	1,1	0,4	12,0	100
Diego Garcia								
Amount	158	47	23	23	16	11	120	414
Percent (%)	38,2	11,4	5,6	5,6	3,9	2,7	29,0	100

This suggests that in Funafuti and Darwin, there are more precipitating days than non-precipitating. However, in Gove, Singapore, Thiruvananthapuram and Diego Garcia the amount of soundings is largest in the PR0 group, suggesting

that there are more fair weather days than days with area-averaged precipitation rates of 5-30 mm/day (PR1-PR5). In Singapore and Diego Garcia, the amount of soundings in the fair weather group (PR0) exceeds that of the precipitation groups (PR1-PR5) by roughly 10 %, in Gove roughly 25 % and in Thiruvananthapuram roughly 54 %. Figure 1 supports the large difference between the amount of soundings in the fair weather group and precipitation groups in Thiruvananthapuram, since it shows that during the southern hemisphere summer, which is also the time window investigated in this study (chapter 3), Thiruvanthapuram obtains the smallest amount of precipitation from all of the stations. An increase in the size of the area from which the area-averaged precipitation is calculated from resulted in larger group sizes in the precipitation groups (PR1-PR5) in Funafuti and smaller in the fair weather group (PR0).

4.2 Temperature and relative humidity in bins of precipitation

For each station the mean vertical profiles of absolute and anomalous RH and anomalous temperature in the different groups was plotted to investigate how precipitation is related to these variables. The RH and temperature anomalies for each group were calculated so that the mean vertical profile of the fair weather group (PR0) was subtracted from the mean vertical profile of each precipitation group (PR1-PR5). Figures 7-11 show the mean vertical profiles of RH (a), the anomalous RH (b), and the anomalous temperature (c) for each different group at each station. RH was chosen since it is interesting to see what kind of RH values there are during fair weather and precipitating periods and how these values differ between the different stations. In addition, it is interesting to see how the vertical profiles of temperature and RH differ between non-precipitating and precipitating periods. Hence, the anomalies were calculated. In this chapter, first the results from Funafuti are investigated in detail after which the results from other stations are discussed and compared to those from Funafuti.

4.2.1 Funafuti

Funafuti is an atoll at only 2 meters above sea level in the tropical western Pacific. Due to its location in the middle of a large ocean, the climate in Funafuti is moist and weather is not affected significantly by the land-sea breeze. Figure 1 shows that Funafuti obtains large amounts of precipitation throughout the year. Due to the large heat capacity of oceans, diurnal cycle in temperature in Funafuti is weak. There are no mountains or other significant topography nearby and therefore, weather is not affected by orography. The fact that the effect of the land-sea breeze, orography and diurnal cycle on weather is minimal, and because the data set from Funafuti in IGRA is large, Funafuti is the most ideal of the stations to study the basic properties of convection. Therefore, we have chosen to discuss the results from this station in detail.

Figure 7 shows the vertical profiles of RH (a), the anomalous RH (b) and the anomalous temperature (c) in the different groups in Funafuti. Figure 7b and 7c show that precipitation is associated with anomalies of RH and temperature in the whole troposphere. The RH anomaly is positive throughout the troposphere (figure 7b). The bins with higher precipitation amounts have larger values of RH anomaly (figure 7b) and temperature anomaly (figure 7c) at almost all levels.

Four separate layers can be distinguished from the RH and temperature profiles in figure 7. These layers are 300-500 hPa, 500-800 hPa, 800-950 hPa and 950-1000 hPa. Between 300 and 500 hPa, RH and temperature show clear dependence on the amount of precipitation. Only 5-10 mm of precipitation (PR1) in one day increases RH on average 10 % relative to RH during fair weather periods (figure 7b). Figure 7b also shows that 10-15 mm of precipitation (PR2) is not enough to cause any significant change compared to 5-10 mm (PR1). When the amount of precipitation increases further, the RH anomaly increases steadily. Temperature in the 300-500 hPa layer, in contrast, doesn't show much sensitivity to either 5-10 mm (PR1) or 10-15 mm (PR2) of precipitation (figure 7c). When the amount of precipitation increases further,

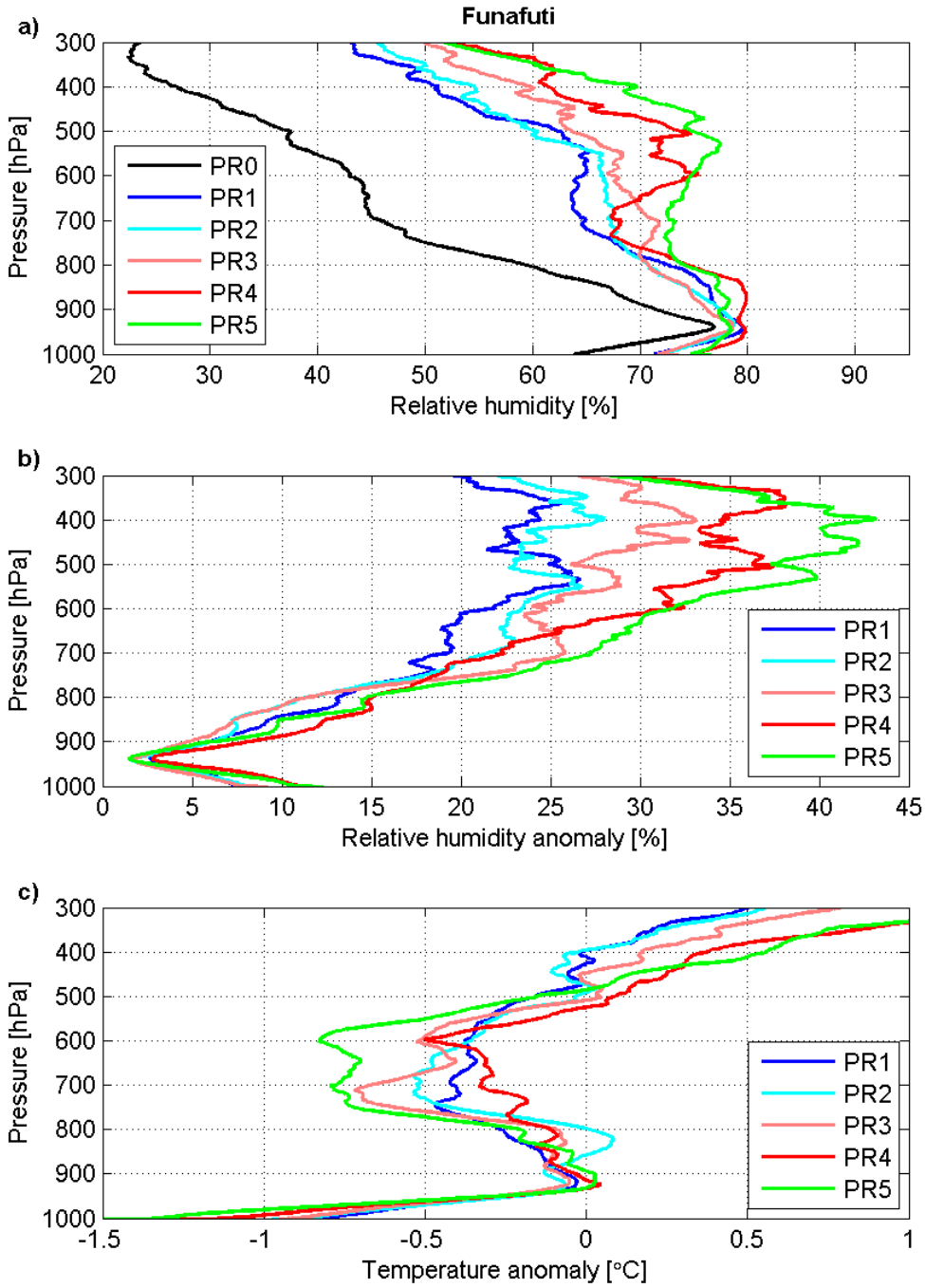

Figure 7. *Mean vertical profiles of a) absolute RH in units of %, b) anomalous RH in units of % and c) anomalous temperature in units of °C obtained from radiosonde measurements from Funafuti in the different groups. The area-averaged precipitation was calculated from a 1°x1° area. Group PR0 (black) is the mean of radiosonde observations conducted after the amount of precipitation during the previous 24 hours was less than 1 mm, PR1 (dark blue) 5-10 mm/day, PR2 (light blue) 10-15 mm/day, PR3 (purple) 15-20 mm/day, PR4 (red) 20-25 mm/day and PR5 (green) 25-30 mm/day. The RH and temperature anomalies for*

each group were calculated so that the mean of the fair weather group (PR0) was subtracted from the mean of each precipitation group (PR1-PR5).

temperature anomalies in the 300-500 hPa layer are positive and become even more positive with higher amounts of precipitation.

As explained in chapter 2, the lower boundary of the anvil cloud in MCSs is usually located roughly between 500 and 600 hPa. Chapter 2 also explained that the anvil cloud induces a positive temperature anomaly in the upper troposphere due to diabatic heating as water vapour condenses to form cloud droplets and precipitation. The relatively moist and warm air in the 300-500 hPa layer in the precipitation groups in figures 7b and 7c is therefore most likely associated with condensation. Figures 7b and 7c suggest that the effect of condensational heating is stronger with higher amount of precipitation.

Between 500 and 800 hPa, RH in the precipitation groups (PR1-PR5) is higher (figure 7b) and temperature smaller (figure 7c) than in the fair weather groups (PR0). Similar to the 300-500 hPa layer, RH in the 500-800 hPa layer is higher with higher amounts of precipitation (figure 7a) but the RH anomalies are smaller in the 500-800 hPa layer than in the 300-500 hPa layer (figure 7b). With the exception of the group with 20-25 mm of precipitation (PR4), also the temperature anomaly is larger with higher amount of precipitation (figure 7c). The 500-800 hPa layer is roughly below the anvil cloud, but above the PBL. As explained in chapter 2, precipitation falling from the anvil cloud evaporates in the 500-800 hPa layer. Because evaporation causes moistening and cooling, the RH and temperature anomalies in the 500-800 hPa layer are most likely the result of evaporation of stratiform precipitation falling from the anvil cloud. Figures 7c and 7b could also suggest that evaporation of water droplets from the anvil cloud is stronger with higher amounts of precipitation.

Between 800 and 950 hPa, the positive RH and negative temperature anomalies are smaller than in the 500-800 hPa and 950-1000 hPa layers (figure 7b and 7c). The vertical gradient of the temperature anomaly is largest in the group with the highest amount of precipitation (PR5), but large gradients are also seen

in all precipitation groups (figure 7c). Neither RH nor the temperature anomaly shows increase with higher amount of precipitation in the 800-950 hPa layer (figure 7a and 7c). That the 800-950 hPa layer is warmer than the layer above and below might be the result of adiabatic warming associated with mesoscale unsaturated downdrafts as described in chapter 2.

In the precipitation groups (PR1-PR5), the layer below 950 hPa is dominated by cooler and moister air relative to the fair weather group (PR0, figures 7b and 7c). Chapter 2 described the two downdrafts observed in MCSs by Zipser (1977). The cool and moist air in the lowest layer associated with convective-scale saturated downdrafts in the cumulonimbus region is seen in figures 7b and 7c below 950 hPa. The group with the highest amount of precipitation (PR5) is associated with the coldest air and the group with least precipitation is associated with the warmest air relative to fair weather atmosphere. The temperature anomaly at the surface in the group with the highest amount of precipitation (PR5) is about -1.7°C (not shown) and in the group with the smallest amount of precipitation (PR1) it is about -0.7°C (figure 7c). RH at the surface in the category with the highest amount of precipitation is roughly 77 % and in the fair weather group it is on average 64 % (figure 7a).

These results suggest that between 300-800 hPa, precipitation is associated with larger moisture anomalies than below 800 hPa. The higher the amount of precipitation is, the larger the anomalies of RH and temperature are at most levels. In the lowest layer (below 950 hPa) the effect of convective-scale saturated downdrafts is seen, as they can spread quite far to the surroundings of the convective precipitation area when they reach the surface. Precipitation is associated with RH anomalies of over 40 % (figure 7b) and temperature anomalies of almost 2 °C (not shown). These anomalies are significant in the tropics and can affect subsequent atmospheric processes. This will be discussed in chapter 5.

4.2.2 Other stations

In addition to Funafuti, we produced similar figures as figure 7 for Darwin, Gove, Singapore, Diego Garcia and Thiruvananthapuram. In this chapter we will present the results from these measuring stations. This provides information of the sensitivity of the results from Funafuti to the location in the tropics, what effects are actually associated with precipitation and how the local environment of the station affects the results of this study. The measuring stations are located in different environments: some are on the coast of a continent and some are atolls in the middle of an ocean. The results in Funafuti were discussed in detail and therefore in this chapter we will only compare the results from the abovementioned measuring stations to those of Funafuti.

Darwin

Darwin is located near the northern coast of Australia. Therefore, the climate in Darwin differs from the climate in Funafuti, which is an atoll in the middle of a tropical ocean. Weather in Darwin is affected by land-sea breeze. When wind is from the south, dry continental air is advected from inland. When wind is from the ocean, moist air is advected from the tropical ocean of high SSTs. Because of the effect of land, the diurnal cycle in temperature is significant. There is highland and even some mountains to the west of Darwin. Therefore, depending on whether wind is from the east or from the west, orographic precipitation can modify the weather in Darwin.

Figure 8 shows the vertical profiles of RH (a), the anomalous RH (b) and the anomalous temperature (c) in the different groups in Darwin. The vertical profiles are mostly similar to those of Funafuti (figure 7), but some differences are seen. RH is larger in the precipitation groups (PR1-PR5) than in the fair weather group (PR0, figure 8a). RH anomalies in Darwin are largest in the 300-800 hPa layer and increase systematically with increasing amount of precipitation (figure 8b), similar to Funafuti (figure 7b).

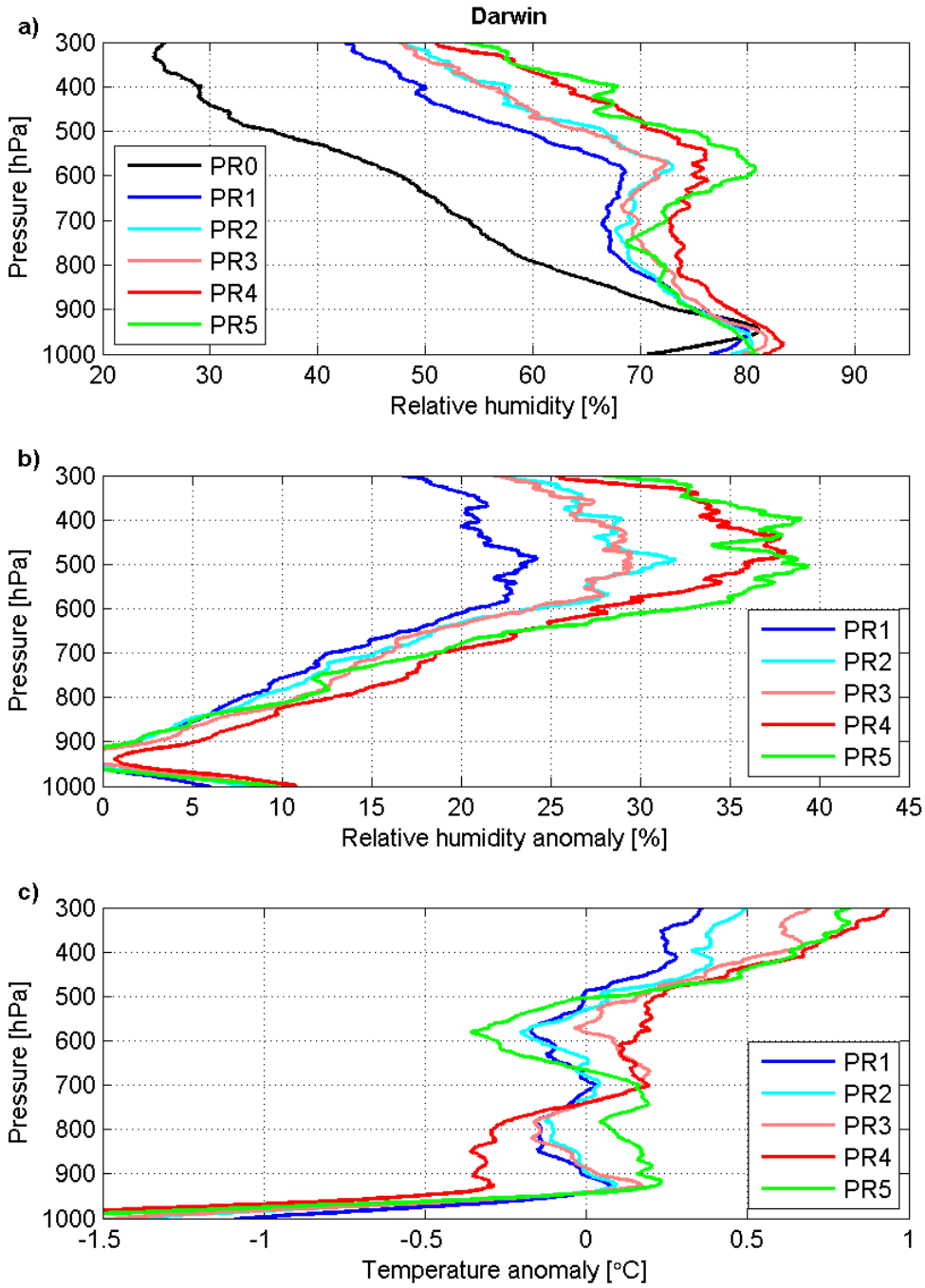

Figure 8. *Same as figure 7 but for Darwin.*

Figure 8b shows that 5-10 mm/day of precipitation (PR1) in Darwin is associated with large RH anomalies in the 300-800 hPa layer. This is similar to Funafuti (figure 7b). However, RH in the group with 15-20 mm/day of precipitation (PR3) does not seem to differ notably from the group with 10-15

mm of precipitation (PR2). RH in the groups with 20-25 (PR4) and 25-30 mm (PR5) of precipitation is larger than in the groups with less precipitation, but the RH values between the two groups with the most precipitation are similar in the upper troposphere. Because RH in Darwin does not increase as systematically with higher amounts of precipitation as in Funafuti, RH in Darwin is not as sensitive to the amount of precipitation as in Funafuti.

In Darwin, the vertical profile of the temperature anomaly (figure 8c) in the first four precipitation groups (PR1-PR4) are different from Funafuti (figure 7c). Figure 8c shows that, in Darwin, the temperature anomaly in the groups with 5-10 (PR1) and 10-15 mm (PR2) of precipitation changes sign at roughly 500 hPa, so that the anomaly is positive above and negative below 500 hPa. This may be due to diabatic heating in the anvil cloud and evaporative cooling below it, but the anomalies are relatively small. The positive temperature anomaly in the group with 15-20 mm (PR3) and 20-25 mm (PR4) of precipitation extends as low as 750 hPa. Therefore, temperature anomalies in these groups do not show clear signals of evaporation of stratiform precipitation in the middle troposphere, even though the RH anomalies are positive in this layer. This is different from the results of Funafuti, which showed clear signals of the relatively cool and moist air in the 500-800 hPa layer (figure 7b and 7c). This could be due to other processes, for example the land-sea breeze, causing larger changes to the temperature field than convection in Darwin.

The anomalous temperature profile in the group with 25-30 mm (PR5) of precipitation is different from the other groups (figure 8c). Four layers can be distinguished with roughly similar features as in Funafuti (figure 7c). Diabatic heating in the anvil cloud is shown as a highly positive temperature anomaly between 300 and 500 hPa in figure 8c. Between 500 and 700 hPa the temperature anomaly is negative due to evaporative cooling of stratiform precipitation. Between 700 and 950 hPa temperature anomaly is again positive. This similar structure, with a decrease in the negative temperature anomaly below the 500-700 hPa layer, was also seen in the profiles of Funafuti in figure 7c, except that in all groups the anomaly was almost always slightly negative.

The layer below 950 hPa in figure 8c shows the effect of convective-scale saturated downdrafts, since this layer is occupied by cooler and moister air in the precipitation groups (PR1-PR5) than in the fair weather group (PR0). That the vertical profile of temperature anomaly has a similar structure to those of Funafuti only in the group with the highest amount of precipitation (PR5) could suggest that the amount of precipitation has to be higher in Darwin than in Funafuti in order for convection to be associated with notable temperature anomalies.

The largest temperature anomaly at the surface is approximately -3.5°C (not shown) and it is associated with the periods of highest amount of precipitation (PR5). This temperature anomaly is also larger than that of Funafuti (not shown). Figure 8a shows that RH at the surface in the fair weather group (PR0) is approximately 71 %. RH increases with higher amounts of precipitation and is roughly 81 % in the group with the highest amount of precipitation (PR5). RH is larger and temperature anomaly more negative at the surface in Darwin (figures 8a and 8c) than in Funafuti (figures 7a and 7c). Therefore, convective-scale saturated downdrafts modify the temperature and humidity of the layer below 950 hPa more effectively in Darwin than in Funafuti.

Gove

Gove is located on the coast of northern Australia to the west of Darwin (figure 5). The climate in Gove is therefore similar to Darwin, and weather is modified significantly by the land-sea breeze and orographic precipitation. According to table 2, over 10 % less soundings fall into the precipitation groups (PR1-PR5) of Gove than Darwin, and over 18 % more fall into the fair weather group (PR0). This suggests that Gove experiences less precipitating days than Darwin, which can be partly due to the highland between the two stations.

Figure 9 shows the vertical profiles of RH (a), the anomalous RH (b) and the anomalous temperature (c) in Gove. Figure 9b shows that RH is higher in the precipitation groups (PR1-PR5) than in the fair weather group (PR0) and that

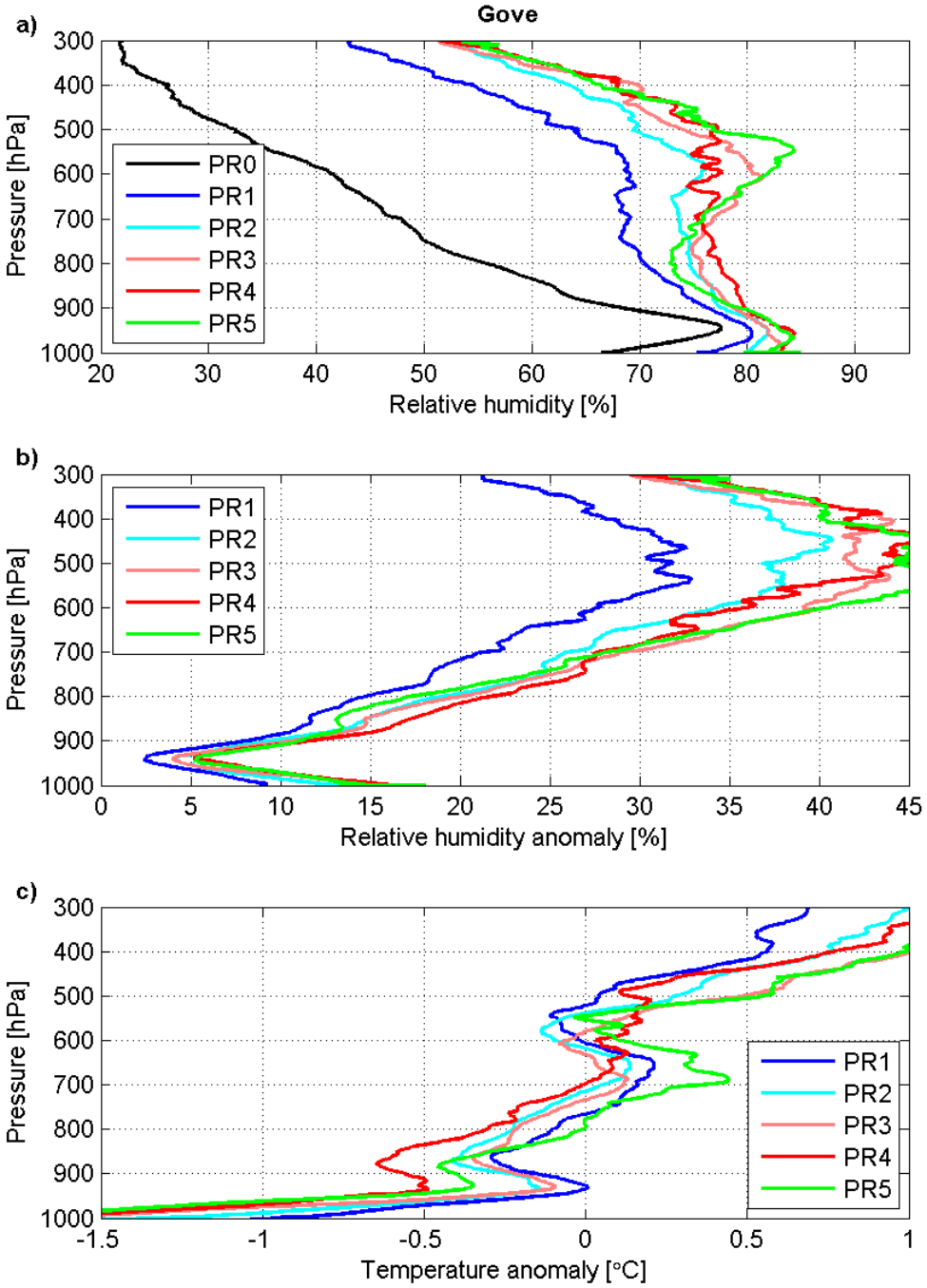

Figure 9. *Same as figures 7 and 8 but for Gove.*

RH is higher with higher amounts of precipitation at almost all levels. This is similar to what was observed in Funafuti (figure 7). RH in Gove is more sensitive to the amount of precipitation in the 300-800 hPa layer compared to below 800 hPa. Diabatic heating and moistening in the anvil cloud is visible in

figures 9b and 9c as positive RH and temperature anomalies in the 300-500 hPa layer. Convective-scale saturated downdrafts modify the layer below 950 hPa so that this layer is occupied by cool and moist air in the precipitation groups (PR1-PR5, figure 9c). These features are similar to both Funafuti (figure 7) and Darwin (figure 8), although the negative temperature anomalies at the surface in Gove are larger than in Funafuti (not shown).

Above 900 hPa, RH anomalies are larger in Gove (figure 9b) than in Funafuti (figure 7b). Figure 9b shows that, in the 300-800 hPa layer, even 5-10 mm of precipitation (PR1) is associated with over 30 % change in RH. RH in the group with the highest amount of precipitation (PR5) differs from the fair weather group by over 45 % at its highest. The RH anomalies are roughly 10 % larger than in Funafuti (figure 7b). The differences in the anomalies are the result of smaller RH in the fair weather group (PR0) and larger RH in the precipitation groups (PR1-PR5) in Gove relative to Funafuti. Therefore, in non-precipitating situations, the free-troposphere is, on average, drier in Gove than in Funafuti. This is reasonable, since Funafuti is located in the middle of a tropical ocean and Gove on the coast of a large continent. The same amount of precipitation is associated with a moister atmosphere in Gove than in Funafuti.

No signals of evaporative cooling of stratiform precipitation in Gove is seen in figure 9c. The temperature anomalies in all groups change sign between 700 and 800 hPa, so that above this layer the anomalies are positive. This behavior is similar to the four first precipitation groups of Darwin (figure 8c).

Singapore

Singapore is the nearest station to the equator investigated in this study. The location near the equator on a maritime continent means that no clear seasons can be distinguished. Singapore is heavily urbanized, which affects the weather significantly since temperatures near heavy urbanization are observed to be higher than temperatures far away (Chow and Roth 2006).

Figure 10 is the same as figures 7, 8 and 9 but for Singapore. Also in Singapore, RH is larger in the precipitation groups (PR1-PR5) than in the fair weather group (PR0) and RH increases with higher amounts of precipitation (figure 10a). RH in each group in Singapore (figure 10a) is larger than in those of Funafuti (figure 7a). The atmosphere is therefore, on average, moister in Singapore than in Funafuti. Figure 10a shows that RH at the surface exceeds 80 % even during fair weather periods, whereas in Funafuti it is about 64 % (figure 7a). The spread in the RH anomalies between different precipitation groups above the 800 hPa pressure level is smaller in Singapore (figure 10b) than in Funafuti (figure 7b). Therefore, RH depends on the amount of precipitation less in Singapore than in Funafuti.

The anomalous temperature profiles of Singapore (figure 10c) are quite similar to those of Funafuti (figure 7c). Positive temperature anomalies associated with diabatic heating in the anvil cloud are seen above 500 hPa in all groups in figure 10c. Below 500 hPa is a layer of negative temperature anomalies suggesting the presence of diabatic cooling due to evaporation of stratiform precipitation. Cooling is largest between 500 and 700 hPa and below 700 hPa the negative temperature anomaly decreases in all groups, similar as in Funafuti.

The temperature anomaly at the surface is about -0.4°C in the group with the highest amount of precipitation (PR5), and about 0.2°C in the group with the smallest amount of precipitation (PR1, figure 10c). The temperature anomalies at the surface are smaller in Singapore than in Funafuti (figure 7c) and therefore the effect of convective-scale saturated downdrafts is weaker in Singapore than in Funafuti.

Thiruvananthapuram

Thiruvananthapuram is located in the southern part of India. Figure 1 shows that this region obtains less precipitation than the other stations observed in this study. The location on the coast of a large continent means that weather is affected by the land-sea breeze and diurnal variation in temperature

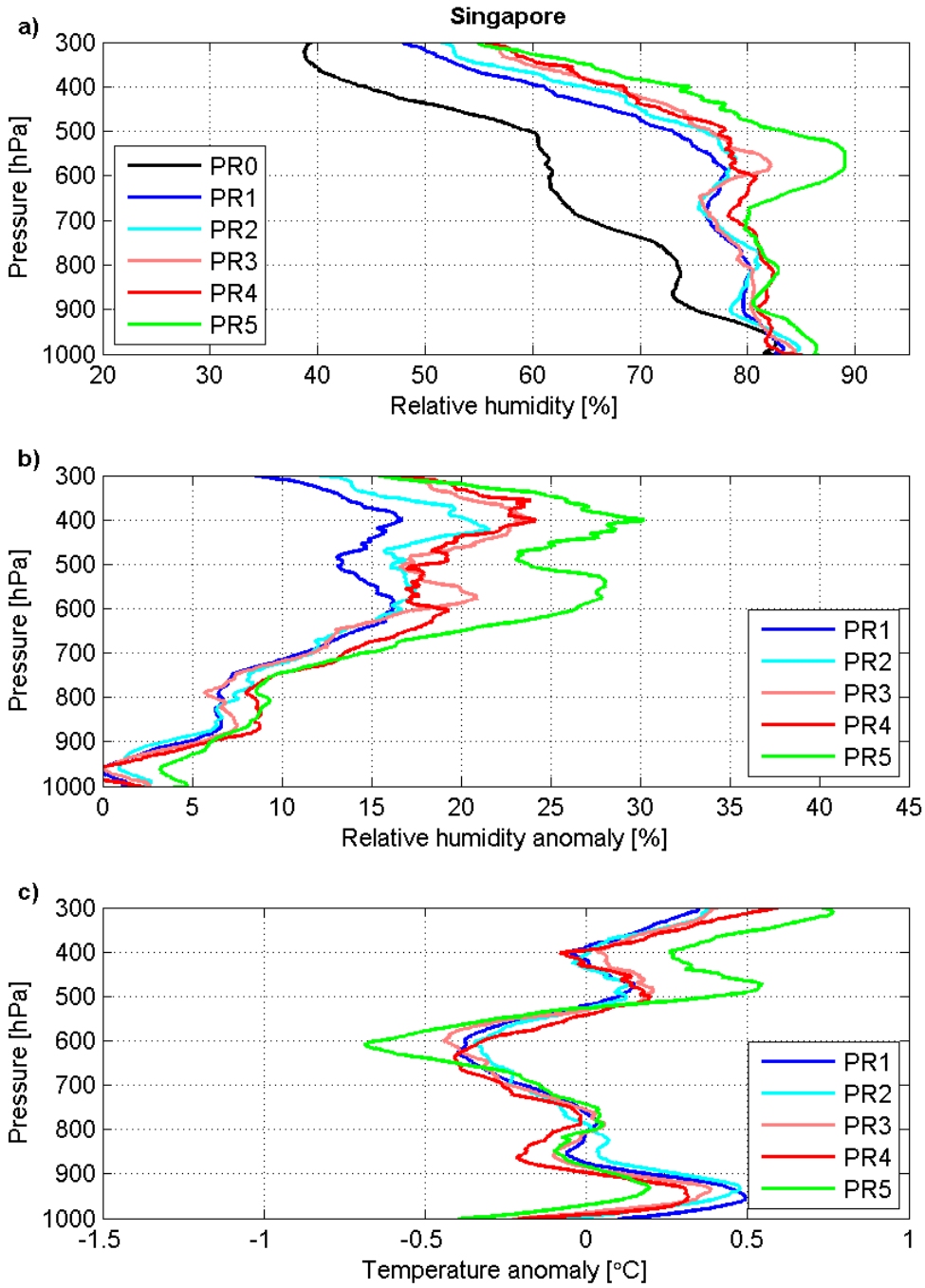

Figure 10. *Same as figures 7, 8 and 9 but for Singapore.*

can be significant. Also monsoon convection has an impact on the climate of Thiruvanathapuram.

Results from Thiruvananthapuram indicate that also at this station, precipitation is associated with positive RH anomalies throughout the troposphere (figure 11b). Almost throughout the troposphere, RH in the precipitation groups is smallest in the group with 5-10 mm of precipitation (PR1) and largest with 20-25 mm of precipitation (PR4, figure 11a). The small amount of data in the group with 25-30 mm of precipitation (PR5, table 2) results in significant noise in the RH and temperature profiles and therefore it is difficult to draw any meaningful conclusions about this group. The RH anomalies in Thiruvananthapuram (figure 11b) peak lower in the troposphere than in Funafuti (figure 7b). Figure 11b shows that the largest RH anomaly and spread between the anomalies is between 600 and 700 hPa. Above and below this layer the spread is smaller. Figure 11a shows that RH at the surface exceeds 80 % in all of the precipitation groups, which is larger than in those of Funafuti (figure 7a).

Temperature anomalies are always negative in Thiruvananthapuram, except in the groups with 5-10 mm (PR1), 10-15 mm (PR2) and 15-20 mm (PR3) of precipitation in the highest 50 hPa layer (figure 11c). The troposphere is therefore always colder in the precipitation groups (PR1-PR5) than in the fair weather group (PR0). No clear relationship with the amount of precipitation and temperature anomalies is seen in figure 11c. However, in all groups, the coldest air is located between 500-800 hPa, which could indicate the presence of evaporative cooling. Between 800 and 950 hPa is a sign of the relatively warmer layer in the vertical dimension also seen in Funafuti in figure 7c, because in all groups the negative temperature anomaly is smaller in the 800-950 hPa layer. The effect of convective-scale saturated downdrafts below 950 hPa is larger in Thiruvananthapuram than in Funafuti. Below 950 hPa, the negative temperature anomalies in Thiruvananthapuram are larger than in Funafuti (not shown).

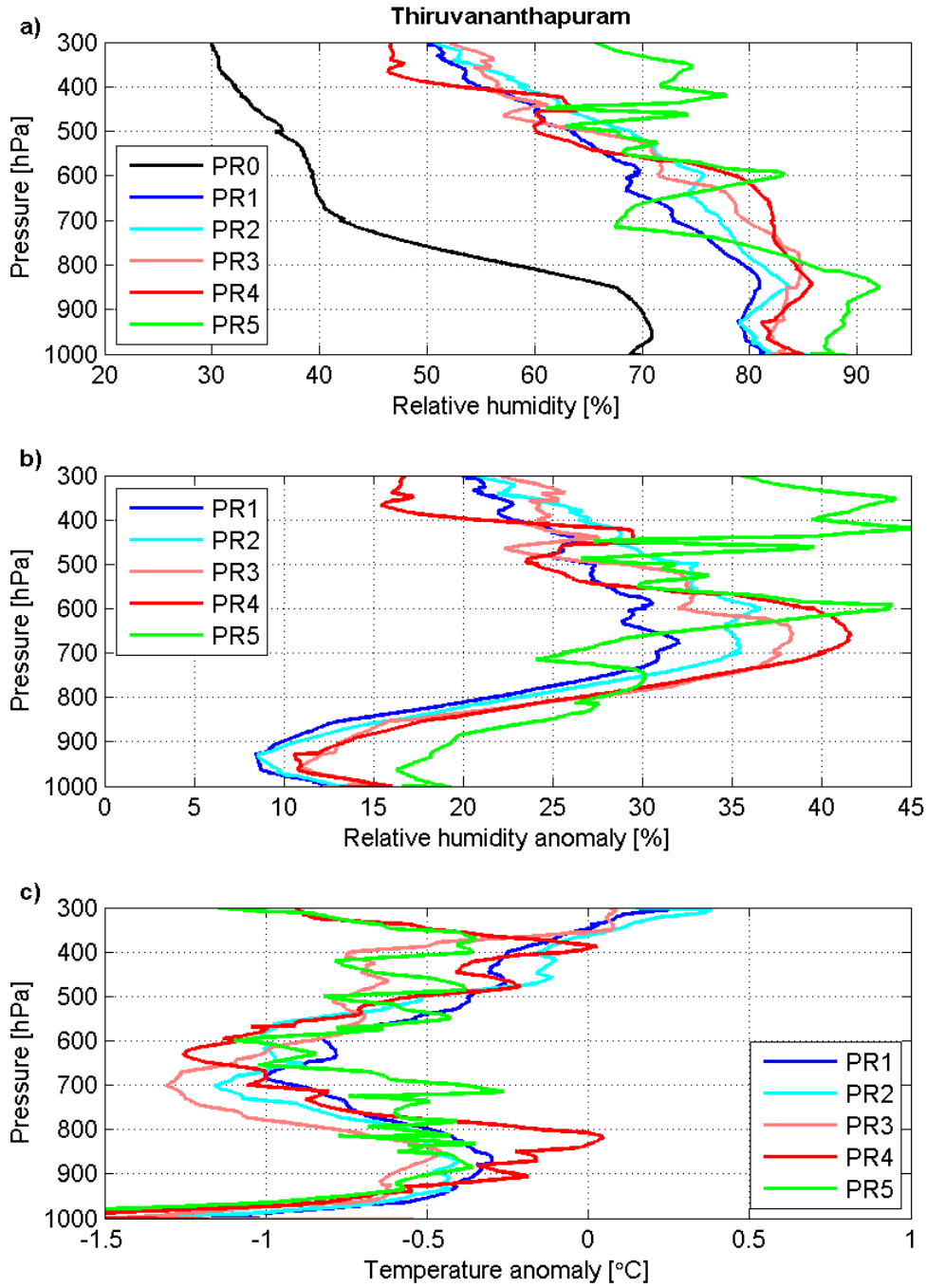

Figure 11. *Same as figures 7, 8, 9 and 10 but for Thiruvanathapuram.*

Diego Garcia

Similar to Funafuti, Diego Garcia is an atoll, but Diego Garcia is located in the eastern Indian Ocean. The climate in Diego Garcia is therefore similar to the

climate of Funafuti (section 4.2.1). The mean vertical profiles of temperature and RH in Diego Garcia (figure 12) are noisy, since the amount of data is small (table 2). However, some interesting features are visible in figure 12. Figure 12a shows that, similar to the other stations, precipitation is associated with a positive RH anomaly and that the RH anomaly is larger in the 300-800 hPa layer than below 800 hPa. However, no clear increase in RH (figure 12b) or temperature (figure 12c) anomaly is seen with higher amounts of precipitation.

The vertical profiles of anomalous temperature in Diego Garcia (figure 12c) are of similar shape as in Funafuti (figure 7c). Figure 12c shows that, in the upper troposphere, temperature anomalies change towards positive values with increasing altitude, although the anomalies in the first four precipitation groups (PR1-PR4) are negative at almost all altitudes. The coldest air is located between 500-800 hPa, perhaps due to evaporative cooling. It is interesting that also at this station, even though the results are quite noisy, a relatively warm layer in the vertical dimension is visible between 800 and 950 hPa, which is similar to the other stations. The layer below 950 hPa is occupied by cool and moist air, similar to the other stations. Temperature anomalies at the surface are of roughly similar size to those of Funafuti (not shown).

4.3 Sensitivity of results to area chosen

Section 4.1 concentrated on the results from binning the data with area-averaged precipitation over an area of 1°x1°. Because the scale of MCSs can exceed 1°, the sensitivity of the results to the size of the area from which area-averaged precipitation is calculated from was studied. In this chapter the results from averaging precipitation over a 5°x5° area in Funafuti are discussed.

Figure 13 shows the vertical profiles of absolute (a) and anomalous RH (b) and anomalous temperature (c) in each group in Funafuti similar to figure 7. Figure 13 shows that, also in the 5°x5° case, precipitation is associated with positive RH anomalies (figure 13a) and the RH and temperature anomalies are larger with higher amounts of precipitation (figures 13b and 13c). The vertical profiles

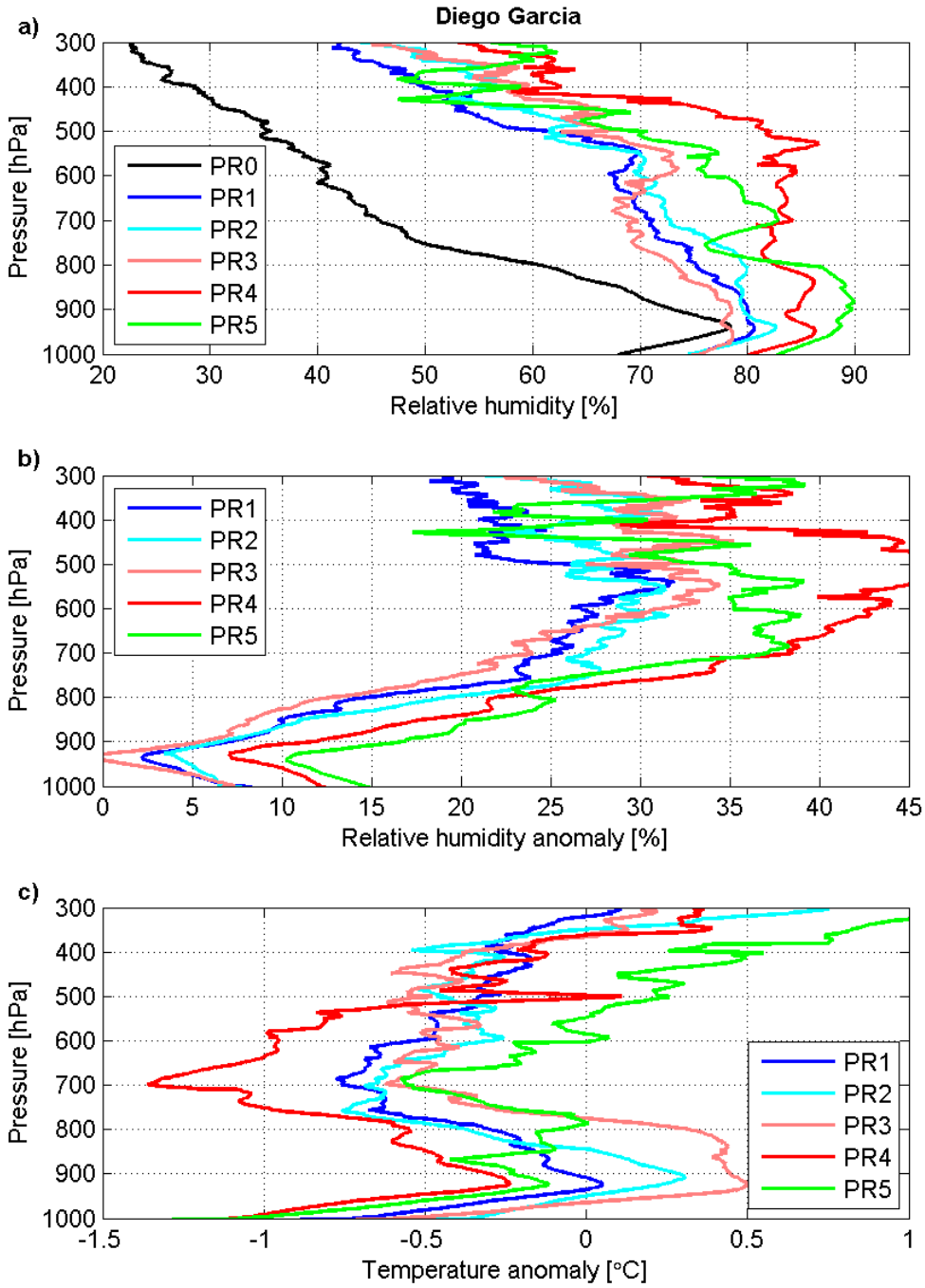

Figure 12. *Same as figure 7, 8, 9, 10 and 11 but for Diego Garcia.*

of temperature and RH are of the same shape in the 5°x5° (figure 13) than in 1°x1° case (figure 7). There are signals of diabatic heating within the anvil cloud (above 500 hPa, figure 13c) due to condensation, diabatic cooling below the anvil cloud (below 500 hPa, figure 13c) possibly due to evaporation of

stratiform precipitation and convective-scale saturated downdrafts bringing cool and moist air to the lowest layer (below 950 hPa, figures 13b and 13c). Figure 13b shows that RH above 800 hPa depends on the amount of precipitation and below 800 hPa no significant relationship between RH and the amount of precipitation is seen, even though RH is somewhat larger in the precipitation groups (PR1-PR5) than in the fair weather group (PR0). These are similar to the 1°x1° case.

Some differences are visible between the 1°x1° (figure 7) and 5°x5° (figure 13) cases. When the amount of precipitation increases from 5-10 mm (PR1) to 10-15 mm (PR2) and then to 15-20 mm (PR3), RH above 800 hPa increases systematically (figures 13a and 13b). Figure 13b shows that 15-20 mm of precipitation (PR3) is associated with RH anomalies of over 40 % in the upper troposphere, but after this amount, RH does not systematically increase with higher amounts of precipitation (PR4 and PR5), which is different from the 1°x1° case (figure 7b). Temperature anomalies in the 500-800 hPa layer are of similar size in the 5°x5° case (figure 13c) than in the 1°x1° case (figure 7c). However, the temperature anomaly does not depend on the amount of precipitation as much in the 5°x5° case as in the 1°x1° case. The 800-950 hPa layer is characterized by warmer air than in the 500-800 hPa layer and in the layer below 950 hPa, similar as in the 1°x1° case. However, figure 13c shows that, in all precipitation groups (PR1-PR5), the gradient in the temperature anomaly between the 500-800 hPa and the 800-950 hPa layer is stronger in the 5°x5 case than in the 1°x1° case (figure 7c). The temperature anomaly in some of the precipitation groups, particularly in the group with the highest amount of precipitation (PR5), is positive in the 800-950 hPa layer. Even though there are some differences between the 1°x1° and 5°x5° cases, they are so minor that the results suggest that no strong sensitivity to the size of the area is seen when comparing figures 7 and 13.

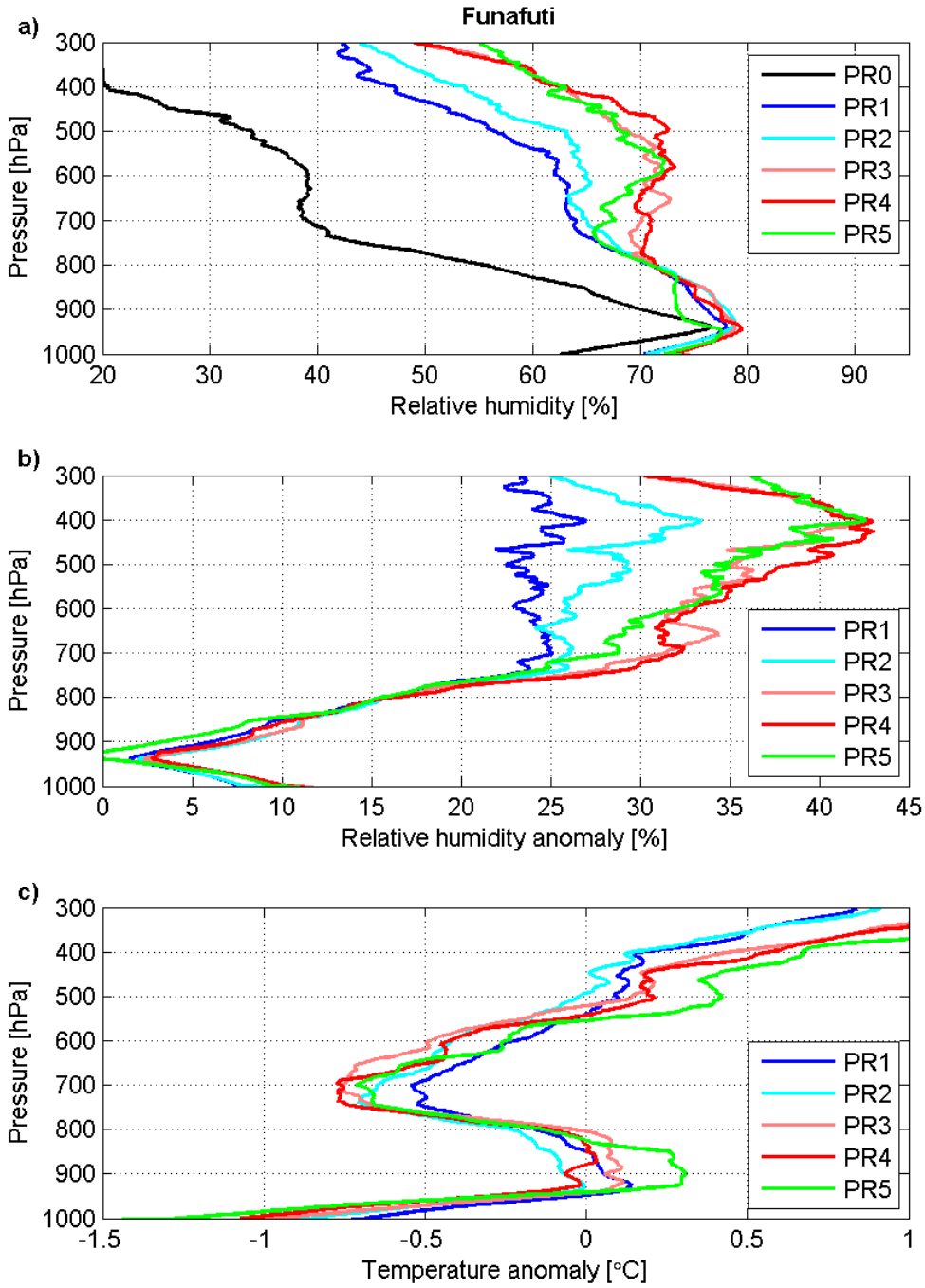

Figure 13. *Same as figure 7 but for area-averaged precipitation from a 5°x5° area.*

4.4 Advection by the horizontal wind

In addition to plotting the vertical profiles of temperature and RH, the vertical profiles of horizontal wind speed were plotted for each station (figure 14).

Visualizing the vertical profiles of wind speed yields information of the intensity of advection by the horizontal wind. Large wind speeds can affect the vertical profiles of temperature and RH presented in section 4.2. Figure 14 shows that, above 800-900 hPa, wind speeds in all groups are over 5 ms^{-1} at almost all levels and at all stations. Wind speeds are smaller below 800-900 hPa. In Funafuti (figure 14a), Darwin (figure 14b) and Gove (figure 14c), largest wind speeds are about 9-10 ms^{-1} in magnitude and in Thiruvananthapuram (figure 14e) and Diego Garcia (figure 14f) wind speeds exceed 11 ms^{-1}. In Singapore (figure 14d), wind speeds are roughly 5-7 ms^{-1} at all levels in the 300-800 hPa.

Mean wind speed of 5 ms^{-1} transports air parcels over 400 km in 24 hours and wind speeds as high as 10 ms^{-1} over 850 km. In section 4.2, one assumes that the air observed by the radiosonde represents air affected by precipitation, since the purpose of this study is to investigate the relationship between precipitation and RH/temperature. However, large wind speeds might advect the air affected by precipitation so that the radiosonde does not measure air affected by precipitation. Therefore, because wind speeds are large, advection of the horizontal wind may have influenced the observed temperature and RH anomalies presented in section 4.2. To quantify the effect of advection on the results obtained in this study, we could further subset the soundings based on the magnitude of the wind speed. However, no meaningful conclusions can be made from subsetting the soundings based on wind speed, since the amount of data is small.

5 DISCUSSION

The results obtained in this study suggest that precipitation and processes within MCSs are associated with anomalies of temperature and RH throughout the troposphere. The results from each station suggest almost similarly structured temperature and RH anomalies, which were calculated by subtracting the mean vertical temperature and RH profiles of the non-precipitating group from those of the groups with certain amount of precipitation, although some differences are distinguished between the stations.

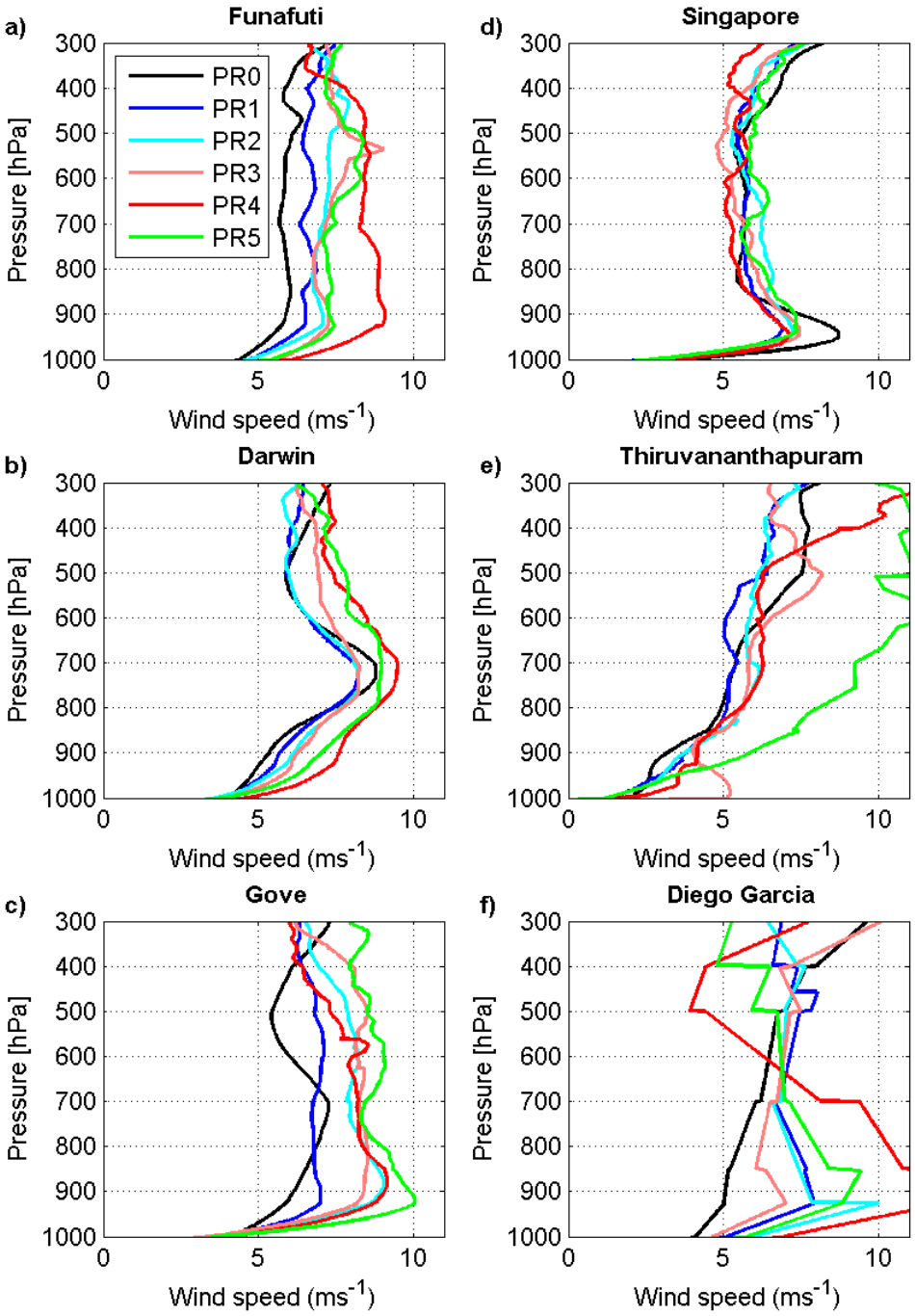

Figure 14. *Vertical profiles of mean horizontal wind speed in the PR0-PR5 groups in a) Funafuti, b) Darwin, c) Gove, d) Singapore, e) Thiruvananthapuram and f) Diego Garcia. Area-averaged precipitation is calculated from a 1°x1° area.*

The results suggest that precipitation is associated with a positive RH anomaly throughout the whole troposphere, the RH anomaly is largest above 800 hPa and higher amount of precipitation is associated with a more humid

atmosphere. This study also shows for the first time that precipitation is associated with a complex vertical temperature anomaly structure. RH anomalies above 800 hPa are largest in Gove (figure 9b) and in Thiruvananthapuram (figure 11b). Convective-scale saturated downdrafts modify the temperature below 950 hPa most effectively in Darwin (figure 8c), Gove (figure 9c) and Thiruvananthapuram (figure 11c), since the temperature anomalies at the surface are largest at these stations. Gove and Thiruvananthapuram are located on the coasts of large continents and further away from the equator than the other stations (figure 5). The climate at these stations is therefore relatively dry and they experience less precipitating days than the other stations (table 2). Therefore, the results obtained in this study suggest that precipitation induces larger temperature and RH anomalies in drier climates.

The effect of precipitation on humidity has been the subject of few other studies. Therefore, it is reasonable to discuss how the results of this study relate to those from a few previous studies. This discussion is provided in section 5.1. The aim of this study is to understand how convection occurring as MCSs, both squall line and disorganized MCSs, influences the vertical profiles of temperature and RH in the troposphere. The initial motivation for this was to understand how deep convection, through induced changes in the vertical profiles of temperature and humidity, might affect the behavior of subsequent deep convection. Although we have not investigated any causal connections between the temperature and RH anomalies and subsequent deep convection in this study, some conclusions can be made based on knowledge of what factors affect the formation and intensity of deep convection and how. A discussion of the relationship between the anomalies of temperature and RH and subsequent convection is provided in section 5.2.

5.1 Humidity anomalies associated with precipitation in other studies

Also other studies have investigated the relationship between precipitation and the humidity of the atmosphere (Holloway and Neelin 2009, Sobel et al. 2004).

Holloway and Neelin (2009) studied the effect of precipitation on humidity by conditionally averaging vertical profiles of specific humidity (q) based on precipitation. Their method is similar to that used in this study, except that they used 1 hour average precipitation rates and q as the humidity quantity. Their results suggest that q is larger during precipitating periods than during non-precipitating periods, and that q increases with higher amounts of precipitation at almost all levels. They also observed that free-tropospheric humidity increases more than humidity in the PBL with higher amounts of precipitation. Sobel et al. (2004) studied lag correlations between rainfall and RH which showed higher lower-tropospheric RH before rain and higher upper-tropospheric RH after it. Therefore, they concluded that higher upper-tropospheric RH is a response to deep convection. The results obtained in this study, that precipitation is associated with a positive RH anomaly especially in the upper-troposphere, that the RH anomalies are largest in the free-troposphere and that higher amount of precipitation is associated with a more humid atmosphere are therefore supported by the results of Holloway and Neelin (2009) and Sobel et al. (2004).

5.2 Effect of temperature and relative humidity anomalies on subsequent convection

The formation and intensity of tropical deep convection is the result of several different factors. That one favorable factor is occurring does not mean that deep convection will commence if detrimental factors are in place, or that one detrimental factor always means that no convection can occur even if the atmospheric conditions are otherwise favorable for the formation of convection.

According to classical convection theory, deep convection depends on the temperature and humidity in the PBL as well as temperature in the free-troposphere (Bister 2014). Cold and unstable air in the free-troposphere increases the amount of convective available potential energy (CAPE) and cold air in the lower troposphere decreases the convective inhibition (CIN). Large CAPE and small CIN are known to be favorable for deep convection. Therefore,

based on this theory, the warm anomaly observed in the upper troposphere associated with precipitation would be detrimental for deep convection because it decreases the amount of CAPE, whereas the cold anomaly in the low-to-middle -troposphere due to evaporative cooling would favor deep convection because it increases CAPE and decreases CIN. The cold air near the surface, the result of convective-scale saturated downdrafts, is unfavorable for deep convection.

In addition to this, several observational and modeling studies have investigated the sensitivity of deep moist convection to free-tropospheric humidity (Neelin et al. 2009, Holloway and Neelin 2009, Derbyshire et al. 2004, Sobel et al. 2004, Bretherton et al. 2004, James and Markowski 2010). Derbyshire et al. (2004) studied the sensitivity of moist convection to mid-tropospheric humidity with a cloud-resolving model and parallel single-column model and concluded that deep convection occurred in the more moist cases and shallow convection occurred in the driest simulation. Bretherton et al. (2004) used satellite observations and showed that precipitation over tropical oceanic regions depended crucially on the saturation deficit of the air column. Saturation deficit describes the difference between the actual and saturation vapor pressure of a volume of air. Sobel et al. (2004) studied the large-scale behavior of the atmosphere during TOGA COARE. Their lag correlations suggest that higher lower-tropospheric RH was favorable for subsequent convection. Many other studies have resulted in the same conclusion, that free-tropospheric humidity plays an important role in the behavior of tropical deep convection. James and Markowski (2010) conducted numerical simulations of quasi-linear convective systems to investigate the sensitivity of deep convective storms to dry air aloft. They found that when CAPE was large, dry air aloft did not have significant effect on deep convection. When CAPE was small, convection required a humid environment. Because over tropical oceans CAPE has been observed to be relatively small, the results of James and Markowski suggest that, especially in the tropics, humidity in the free-troposphere plays an important role in the behavior of deep convection.

Therefore, all processes that increase the free-tropospheric humidity can have important effect on subsequent convection. Because the results of this and other studies suggest that precipitation is associated with larger free-tropospheric RH relative to non-precipitating periods, deep precipitating convection may have important effect on the behavior of subsequent convection. The results of this study suggest that higher amount of precipitation is associated with larger RH, so higher amount of precipitation may be associated with stronger effects on subsequent convection. Because the temperature and amount of moisture in the free-troposphere depends on the amount of precipitation, Bretherton et al. (2004) suggested that deep convective parameterizations that use a fixed reference relative humidity profile should adjust the reference profile to depend on precipitation. They concluded that this might improve the performance of convective parameterizations.

6 SUMMARY

This study has investigated the association of tropical deep convection with the vertical profiles of temperature and RH over tropical oceans. Six weather stations were selected and they are located in Funafuti, Darwin, Gove, Singapore, Thiruvananthapuram and Diego Garcia. The vertical profiles of temperature, RH and horizontal wind speed were constructed by interpolating linearly between every 1 hPa of daytime radiosonde observations from the IGRA database. The profiles were then binned into six categories based on the amount of area-averaged precipitation obtained during the preceding 24 hours before the radiosonde observation. The area-averaged TRMM-based precipitation rates were calculated from areas of 1°x1° and 5°x5° so that the station was in the centre of the area. One of the groups contained soundings where the amount of area-averaged precipitation was less than 1 mm (PR0). This group represents non-precipitating atmosphere. The other groups were defined so that a certain amount of area-averaged precipitation had occurred (PR1-PR5). In each group, a mean of observations at each level was taken. Thus, for each station and each group, a mean vertical profile of RH, RH anomaly, temperature anomaly and wind speed was formed. The anomalies for each

group were calculated by subtracting the mean vertical profiles of temperature and RH of a group with no precipitation (PR0) from the vertical profiles of a group with precipitation (PR1-PR5).

First the results from averaging precipitation from a 1°x1° area was studied. The vertical profiles of RH, RH anomaly and temperature anomaly at each station were presented to understand how precipitation is associated with temperature and RH in the troposphere. The results suggest that precipitation is associated with a positive RH anomaly in the whole troposphere, the positive RH anomaly is largest in the free-troposphere and higher amounts of precipitation are associated with larger RH and temperature anomalies at almost all levels.

Four separate layers were distinguished from the vertical profiles of temperature anomaly and they are approximately 300-500 hPa, 500-800 hPa, 800-950 hPa, 950-1000 hPa. Figure 15 summarizes the main characteristics of these layers and what processes they are most likely associated with. In the 300-500 hPa layer, anomalies of temperature and RH were mainly positive. According to observations made by Zipser (1977), the lower boundary of the anvil cloud in MCSs is located between roughly 500-600 hPa. Therefore, the warm and moist anomaly above 500 hPa is most likely due to diabatic heating associated with condensation of water vapor to form cloud and rain droplets. Below the anvil cloud, between 500-800 hPa, is a cooler and moister layer during precipitating periods most likely associated with diabatic cooling due to evaporation of stratiform precipitation falling from the anvil cloud. Between 800-950 hPa the negative temperature anomalies and positive RH anomalies are smaller than in the 500-800 hPa and 950-1000 hPa layers. This may be due to the effect of mesoscale unsaturated downdrafts. The layer below 950 hPa is occupied by cooler and moister air during precipitating periods, likely due to the effect of convective-scale saturated downdrafts induced by intense precipitation from the deep convective areas of MCSs. These results show for the first time that precipitation is associated a complex vertical temperature anomaly structure.

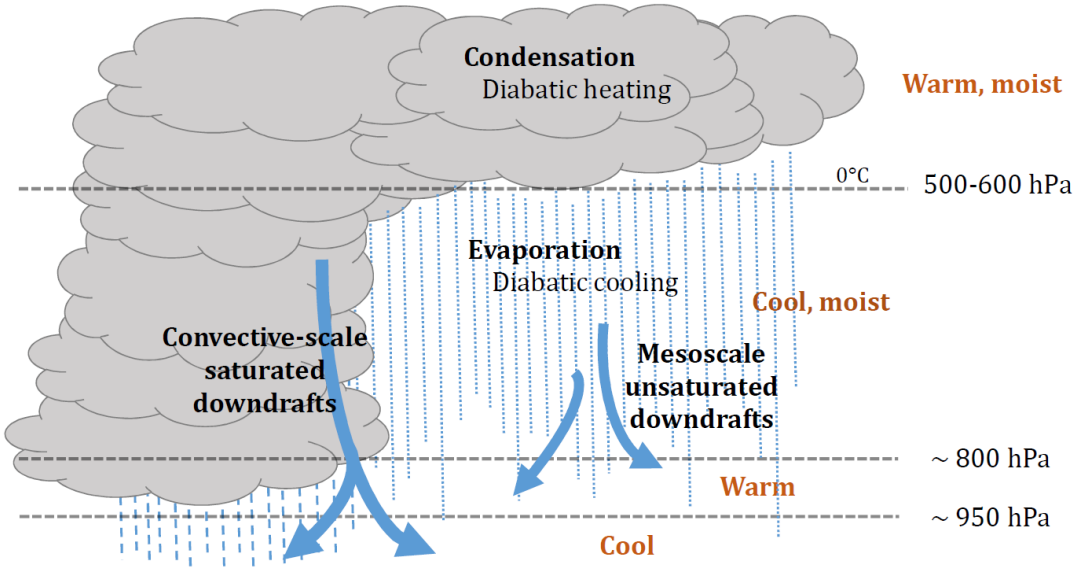

Figure 15. *Summary of the temperature and RH anomalies associated with MCSs. Black colors indicate the processes that are hypothesized to affect the characteristics of the different layers. Orange colors indicate the observed characteristics of the different layers separated with dashed lines. The 300-500 hPa layer is occupied by warm and moist air during precipitating periods, the 500-800 hPa layer by cool and moist air, the 800-950 hPa layer by warmer air with respect to the 300-500 hPa and 950-1000 hPa layers and the 950-1000 hPa layer by cool air.*

The sensitivity of the results to the size of the area from where precipitation was calculated was studied by binning the data according to area-averaged precipitation from an area of 5°x5° in Funafuti. The results showed no significant sensitivity to the size of the area. An investigation of the vertical profiles of horizontal wind speed showed that wind speeds were, on average, large in the free-troposphere. Therefore, advection of air by the horizontal wind was large and the radiosonde observation may not have measured air affected by precipitation. The horizontal wind may have influenced the observed temperature and RH anomalies.

Having larger datasets would have been more favorable. The amount of data at some stations was small and resulted in significant amount of noise in the results. The time resolution of this study was 24 hours, since the radiosonde measurements from the stations were available mostly every 24 hours. Using a smaller time resolution would have enabled a study of the causal connection

between deep convection and the vertical profiles of RH and temperature. This work will continue with analysis of precipitation and radiosonde observations using a smaller time resolution and different data set.

ACKNOWLEDGMENTS

This work was funded by the Finnish Academy of Science and Letter's Vilho, Yrjö and Kalle Väisälä Foundation. I would also like to thank Marja Bister and Victoria Sinclair for their guidance and ideas throughout this process and their help with writing this thesis. I would like to thank Heikki Järvinen for reviewing this thesis.

REFERENCES

Bister, M., 2014: Konvektiiviset sääjärjestelmät ja ilmasto. Ilmakehätieteiden osasto. Helsingin Yliopisto.

Bretherton, C. S. and M. E. Peters, and L. E. Back, 2004: Relationships between water vapor path and precipitation over the tropical oceans. *J.Clim.,* **17**, 1517-1528.

Chow, W. T. and M. Roth, 2006: Temporal dynamics of the urban heat island of Singapore. *Int.J.Climatol.,* **26**, 2243-2260.

Derbyshire, S., I. Beau, P. Bechtold, J. Grandpeix, J. Piriou, J. Redelsperger, and P. Soares, 2004: Sensitivity of moist convection to environmental humidity. *Q.J.R.Meteorol.Soc.,* **130**, 3055-3079.

Hartmann, D. L., 1994: *Global physical climatology.* Academic press. San Diego, United States, 411 pp.

Hohenegger, C. and B. Stevens, 2013: Preconditioning deep convection with cumulus congestus. *J. Atmos. Sci.*, **70**, 448–464.

Holloway, C. E. and J. D. Neelin, 2009: Moisture vertical structure, column water vapor, and tropical deep convection. *J.Atmos.Sci.,* **66**, 1665-1683.

Houze, R. A., 1993: *Cloud Dynamics.* Academic Press. San Diego, United States, 573 pp.

James, R. P. and P. M. Markowski, 2010: A numerical investigation of the effects of dry air aloft on deep convection. *Mon.Weather Rev.,* **138**, 140-161.

Kalnay, E., M. Kanamitsu, R. Kistler, W. Collins, D. Deaven, L. Gandin, M. Iredell, S. Saha, G. White, J. Woollen, Y. Zhu, A. Leetmaa, R. Reynolds, M. Chelliah, W. Ebisuzaki, W. Higgins, J. Janowiak, K. C. Mo, C. Ropelewski, J. Wang, Roy Jenne, and D. Joseph, 1996: The NCEP/NCAR 40-Year Reanalysis Project. *Bull. Amer. Meteor. Soc.*, **77**, 437–471.

Lucas, C. and E. J. Zipser, 2000: Environmental variability during TOGA COARE. *J. Atmos. Sci*., 57, 2333–2350.

Mapes, B. E., 1993: Gregarious tropical convection. *J.Atmos.Sci.,* **50**, 2026-2037.

Mapes, B. E. and R. A. Houze Jr, 1995: Diabatic divergence profiles in western Pacific mesoscale convective systems. *J.Atmos.Sci.,* **52**, 1807-1828.

Neelin, J. D., O. Peters, and K. Hales, 2009: The transition to strong convection. *J.Atmos.Sci.,* **66**, 2367-2384.

Rickenbach, T. M. and S. A. Rutledge, 1998: Convection in TOGA COARE: Horizontal scale, morphology, and rainfall production. *J. Atmos. Sci.*, **55**, 2715–2729.

Rogers, R. R., and M. K. Yau, 1989: *A Short Course in Cloud Physics*. 3rd edition. Pergamon Press, 293 pp.

Sobel, A. H., S. E. Yuter, C. S. Bretherton, and G. N. Kiladis, 2004: Large-scale meteorology and deep convection during TRMM KWAJEX*. *Mon.Weather Rev.,* **132**, 422-444.

Zipser, E., 1977: Mesoscale and convective-scale downdrafts as distinct components of squall-line structure. *Mon.Weather Rev.,* **105**, 1568-1589.

ELECTRONIC REFERENCES

ERA-40 Atlas, European Centre for Medium-Range Weather Forecasts (ECMWF), accessed October 2nd 2015. *http://old.ecmwf.int/research/era/ERA-40_Atlas/docs/index.html.*

NCEP/NCAR Reanalyses, NOAA/ESRL Physical Sciences Division, Boulder Colorado, accessed October 2nd 2015, *http://www.esrl.noaa.gov/psd/.*

Integrated Global Radiosonde Archive (IGRA), NOAA National Centers for Environmental Information, accessed October 2nd 2015, *https://www.ncdc.noaa.gov/data-access/weather-balloon/integrated-global-radiosonde-archive.*

Tropical Rainfall Measuring Mission (TRMM), accessed October 2nd 2015, *http://trmm.gsfc.nasa.gov/.*